

# The Impact of Stellar Migration on disk Outskirts

Victor P. Debattista, Rok Roškar, Sarah R. Loebman

**Abstract** Stellar migration, whether due to trapping by transient spirals (churning), or to scattering by non-axisymmetric perturbations, has been proposed to explain the presence of stars in outer disks. After a review of the basic theory, we present compelling, but not yet conclusive, evidence that churning has been important in the outer disks of galaxies with type II (down-bending) profiles, while scattering has produced the outer disks of type III (up-bending) galaxies. In contrast, field galaxies with type I (pure exponential) profiles appear to not have experienced substantial migration. We conclude by suggesting work that would improve our understanding of the origin of outer disks.

## 1 Introduction

By the mid-90s the view of disks that prevailed was that they are truncated at some radius with little or no stars at larger radii. Using photographic images of three edge-on galaxies, van der Kruit (1979) had shown that disks appear sharply truncated. Based on four edge-on galaxies, van der Kruit and Searle (1982) measured truncation radii at  $4.2 \pm 0.6 R_d$ , where  $R_d$  is the scalelength of the disk. In face-on galaxies, van der Kruit (1988) found closely spaced light contours in the outer disks, which he interpreted as the advent of the truncation. van der Kruit (1987) suggested

---

Victor P. Debattista  
Jeremiah Horrocks Institute, University of Central Lancashire, Preston, PR1 2HE, UK, e-mail: vpdebattista@uclan.ac.uk

Rok Roškar  
Research Informatics, Scientific IT Services, ETH Zürich, Weinbergstrasse 11, CH-8092, Zürich, Switzerland, e-mail: rokroskar@gmail.com

Sarah R. Loebman  
Department of Astronomy, University of Michigan, 1085 S. University Ave., Ann Arbor, MI, 48109, USA, e-mail: sloebman@umich.edu

these truncations are the result of detailed angular momentum conservation in the collapse of a uniformly rotating gas sphere. While HI disks are typically larger than the break radius, van der Kruit (2007) showed that HI warps often begin at about the truncation radius. Kregel et al (2002) found truncations in 20 of 34 galaxies with a slightly smaller truncation radius,  $3.6 \pm 0.6 R_d$ . Pohlen et al (2000), on the basis of a sample of 31 edge-on galaxies, revised the mean truncation radius further to  $2.9 \pm 0.7 R_d$  (truncations at 11 – 35 kpc).

Then the picture of disk profiles started changing. Already in NGC 4565 (Naeslund and Joersaeter 1997) and IC 5249 (Byun 1998) a transition from one exponential profile to a steeper one, rather than a sharp truncation, had been found. In his sample of four edge-on galaxies, de Grijs et al (2001) found that truncations are not perfectly sharp. Finally the deep optical imaging of 72 edge-on (Pohlen 2002) and three face-on (Pohlen et al 2002) galaxies firmly established that disk galaxies have broken-exponential profiles, rather than sharp truncations. The transition between the two exponentials has come to be known as a “break”, although the term “truncation” persists. This discovery led to increased interest in disk outskirts because the presence of stars at large radii needed an explanation. The first workshop dedicated to disk outskirts, “Outer edges of disk galaxies: A truncated perspective”, was held at the Lorentz Center in 2005. That same year Erwin et al (2005) identified a new class of disk profiles, the type III “anti-truncated” profiles. The first pure  $N$ -body simulations aimed at producing disk profiles with breaks were presented by Debattista et al (2006), who proposed angular momentum redistribution during bar formation as the cause, while Bournaud et al (2007) and Foyle et al (2008) included also the effect of gas. Roškar et al (2008b) introduced the idea that disk outskirts are populated by stars that have migrated outwards without heating.

A decade later much progress has been made but much more remains to be understood. While generally comprising only a small fraction of the overall stellar mass, disk outskirts are an ideal laboratory for understanding the processes of galaxy formation. These are regions where the dark matter dominates and that are therefore easily perturbed, are generally inhospitable to star formation, and are the interface at which gas, and some satellites, are accreted. In recent years it has become clear that the stars in these regions are generally old. Are these stars the product of ongoing inefficient star formation, or the fossil of a long-ago, efficient, in-situ star formation? Was mass migrated to the outer disk (by bars, clumps, or spirals)? Were the stars accreted from satellites? Understanding which of these processes dominates, and where, provides crucial information on how galaxies formed. This review explores the extent to which stellar migration is responsible for populating the outer disks. In the remainder of this Section we clarify what we mean by profile breaks. In Sect. 2 we review the demographics of different profile types. We introduce stellar migration and angular momentum redistribution in Sect. 3. We then consider each of the profile types in turn in Sect. 4 (type IIs), 5 (type Is), and 6 (type IIIs). Section 7 concludes with suggestions for future directions that can greatly advance our understanding of the origin of stars in outer disks.

## 1.1 Our Definition of Breaks

In the truncated picture of disks, the meaning and location of a truncation is unambiguous. Instead disks do not end abruptly but extend significantly beyond a break. While disks are often well fit by piecewise exponential profiles, the presence of bars, lenses, spirals, rings and asymmetries add bumps and wiggles to profiles. For instance, Laine et al (2014) noted that their galaxies included breaks associated with lenses, with rings, and with star formation breaks. Therefore sometimes it is difficult to assign the location of breaks, particularly if the data being fit are shallow. Such difficulties account for the significant differences in the locations of breaks assigned by different authors. For example, in NGC 4244 the resolved stellar population study of de Jong et al (2007) found a very clear break at  $420''$  while Martín-Navarro et al (2012) found one at  $\sim 290''$  and another at  $\sim 550''$ . Although sharp truncations are not supported by observations, star formation is often observed to be more strongly truncated than the overall mass distribution (Bakos et al 2008). How stars end up past this point is a very important question that gives us insight into important processes that operate in most disk galaxies. With this in mind, this review focuses not on the bumps and wiggles produced by bars, rings, or spirals, but on breaks related to star formation. Thus our primary focus is on type II profiles, which exhibit such breaks, whereas our interest in pure exponential (type I) profiles comes from the absence of these breaks, and in anti-truncated (type III) profiles from their ability to populate the outer disk via some other mechanism.

## 2 Demographics of Profile Type

Stellar disk profiles are piece-wise exponential<sup>1</sup>. This does not imply that the profile of star formation itself must be exponential since even a radially constant star formation rate produces an exponential disk (e.g., Roškar et al 2008b). Why nature prefers exponential disks is uncertain, although many studies have attacked this problem from a variety of perspectives. Whatever the reason, the exponential profile is evidently an attractor. Freeman (1970) identified two types of disk profiles. The first (type I profile) is exponential to the last measured point, while in the second (type II profile) an inner exponential is followed by a steeper one in the outer disk. Erwin et al (2005) extended this classification to include type III profiles, where the outer profile is shallower than the inner one.

Pohlen and Trujillo (2006) found that  $\sim 60\%$  of late-type spirals have a type II profile with the break at  $2.5 \pm 0.6 R_d$  (at  $\mu_r \sim 23.5 \pm 0.8 \text{ mag arcsec}^{-2}$ ), while  $30\%$  have a type III profile, with the break at larger radii,  $4.9 \pm 0.6 R_d$  (at  $\mu_r \sim 24.7 \pm 0.8 \text{ mag arcsec}^{-2}$ ). The mix of profile types varies with Hubble type, with type IIs more frequent in late-type galaxies while type IIIs are more common in early-type galaxies. Erwin et al (2008) found a breakdown of  $27\% : 42\% : 27\%$  for types I : II : III for

<sup>1</sup> Bulges at the centres of galaxies contribute additional light above an exponential.

66 early-type galaxies, with  $\sim 6\%$  having a composite type II+III profile: a type II profile at small radii and a type III further out. Gutiérrez et al (2011), studying 47 face-on early-type unbarred galaxies, found that the type II profiles are more common in late-type galaxies while the type I and III profiles are more common in early-types. By combining all the published studies and accounting for differences in sample definitions, they found global (S0-Sd) frequencies of 21% : 50% : 38% for types I : II : III, with 8% of galaxies having composite II+III profiles. Table 1 presents the fraction of each profile type (with type II+III profiles counted twice) from the combination of these three studies.

	I	II	III
S0-Sb galaxies			
SA	$0.26 \pm 0.07$	$0.14 \pm 0.06$	$0.69 \pm 0.08$
SAB	$0.18 \pm 0.07$	$0.45 \pm 0.09$	$0.48 \pm 0.09$
SB	$0.36 \pm 0.07$	$0.49 \pm 0.07$	$0.20 \pm 0.06$
Sbc-Sd galaxies			
SA	$0.17 \pm 0.08$	$0.52 \pm 0.10$	$0.30 \pm 0.10$
SAB	$0.12 \pm 0.07$	$0.67 \pm 0.10$	$0.21 \pm 0.08$
SB	$0.09 \pm 0.06$	$0.83 \pm 0.08$	$0.09 \pm 0.06$

**Table 1** The fraction of type I, II and III profiles amongst unbarred (SA), weakly barred (SAB) and barred (SB) galaxies. Data for S0-Sb galaxies are from Erwin et al (2008) and Gutiérrez et al (2011). The data for Sbc-Sd galaxies are from Pohlen and Trujillo (2006)

## 2.1 The Role of Environment

Erwin et al (2012) and Roediger et al (2012) found a strong dichotomy between field and Virgo Cluster lenticulars. Both studies found that the fraction of type I profiles rises at the expense of type II profiles. Gutiérrez et al (2011) found type I profiles in one third of lenticular galaxies, with type II profiles uncommon amongst them. Pranger et al (2016) used the Sloan Digital Sky Survey to construct field and cluster samples of  $\sim 100$  galaxies each, in a narrow mass range ( $1 - 4 \times 10^{10} M_{\odot}$ ). They found that type I galaxies are three times more frequent in clusters than in the field. Maltby et al (2012a) came to a very different conclusion, finding roughly half of both their field and cluster samples having a type I profile and only 10% having a type II profile. However, because they concentrated on outer disks through a surface brightness cut at  $24 < \mu < 26.5$  mag arcsec $^{-2}$ , they missed most type II breaks, which are typically brighter. Nevertheless, their fraction of type III profiles is consistent with that of the field sample of Pohlen and Trujillo (2006).

## 2.2 Redshift Evolution

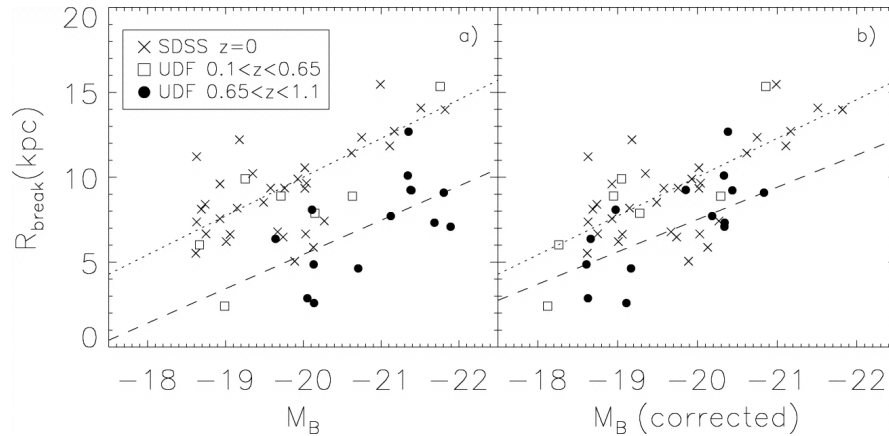


**Fig. 1** Break radius as a function of rest-frame  $B$ -band absolute magnitude for galaxies at different redshift, as indicated in the inset at left. (a) The observed relation. (b) The relation after correcting the absolute magnitude for the mean surface brightness evolution since  $z = 1$ . The dashed lines show the best-fitting relation for the distant sample while the dotted line shows the local relation. Reproduced with permission from Trujillo and Pohlen (2005)

Pérez (2004) found six breaks in a sample of 16 galaxies at  $0.6 \leq z \leq 1.0$ ; the average break radius was  $1.8R_d$ , smaller than in local samples although the detection was biased to smaller radii. In a study of 36 galaxies to  $z \sim 1$ , shown in Fig. 1, Trujillo and Pohlen (2005) found that the location of the breaks, corrected for the mean surface brightness evolution, has increased by 1-3 kpc (25%), while the  $\sim 10\times$  larger sample of Azzollini et al (2008b) found that, at fixed mass, the break radius has increased by a factor  $1.3 \pm 0.1$  since  $z = 1$ .

## 3 Stellar Migration

The breaks in disk profiles are generally at  $2 - 5R_d$  (Pohlen and Trujillo 2006). At these large radii, the surface density is low and the total mass in the outer disk is small. Bakos et al (2008) found that the mass of stars in the outer disk constitutes  $14.7\% \pm 1.2\%$  in type II galaxies and  $9.2\% \pm 1.4\%$  in type III galaxies. Therefore even a quite small transfer of mass from small to large radii can have a significant effect on the overall profile shape. For a pure exponential profile, the total mass outside  $4R_d$  is less than 10% of the total. If just one quarter of the mass between  $R_d$  and  $2R_d$  (i.e.,  $\sim 8\%$  of the total disk mass) is redistributed to radii outside  $4R_d$ , this

nearly doubles the mass at those radii. This means that a galaxy does not need substantial mass redistribution in order for its outer profile to be significantly altered.<sup>2</sup>

### 3.1 Migration via Transient Spirals

The energy in a rotating frame, the Jacobi energy,  $E_J$ , is a conserved quantity:

$$E_J = E - \Omega_p L_z, \quad (1)$$

where  $E$  and  $L_z$  are the energy and angular momenta in the inertial frame, and  $\Omega_p$  is the angular frequency of the rotating frame (Binney and Tremaine 1987).  $E_J$  is a conserved quantity even when the system is not axisymmetric provided the system is viewed in the frame in which the potential is stationary. For a bar or a spiral perturbation, the stationary frame corresponds to the one where  $\Omega_p$  is the pattern speed of the perturbation. Conservation of  $E_J$  requires that changes in angular momentum,  $\Delta L_z$ , and in energy,  $\Delta E$ , are related as  $\Delta E = \Omega_p \Delta L_z$ . For most stars  $\Delta L_z$  averages to zero over an orbit; the exception is for stars at resonances (Lynden-Bell and Kalnajs 1972). The change in angular momentum is accompanied by a change in the radial action,  $J_R$ ; in the epicyclic approximation, this change is given by

$$\Delta J_R = \frac{\Omega_p - \Omega}{\kappa} \Delta L_z, \quad (2)$$

where  $\Omega$  and  $\kappa$  are the angular and radial frequencies of a star. Sellwood and Binney (2002) realised that changes in energy and angular momentum at the corotation resonance (CR), where  $\Omega_p = \Omega$ , are not accompanied by any changes in radial action, and result in no radial heating.

Stars trapped by a spiral at its CR change their energy and angular momentum at fixed  $E_J$  without changing  $J_R$ . Spirals being transient (Sellwood and Carlberg 1984; Sellwood 2011), trapping by a spiral is short-lived, typically lasting for one rotation period. When the spiral decays, trapped stars are released with a different angular momentum than they started with. This is the basis of migration due to corotation-trapping by transient spirals, which Sellwood and Binney (2002) refer to as “churning”. Figure 2 presents an example of churning in a disk with a single strong spiral. The vertical solid lines in the top panels show the location of the CR.

<sup>2</sup> This also poses a challenge for simulations studying the evolution of disk outskirts, which need to minimise noise; for instance initial conditions that are even slightly out of equilibrium can significantly alter the profile at large radii. The most widely used technique for producing initial conditions for simulations assumes Gaussian velocity distributions, which is only an approximate equilibrium. Kazantzidis et al (2004) presented a spectacular example of how this approximation leads to dramatically wrong conclusions in the case of satellite galaxy disruption. The freely available GALACTICS initial conditions code (Kuijken and Dubinski 1995; Widrow and Dubinski 2005; Widrow et al 2008) instead uses the correct distribution function method for setting up galaxies. Likewise, the GALAXY package (Sellwood 2014) includes software for setting up disk galaxies in proper equilibrium.

In spite of the substantial amount of angular momentum exchanges taking place around the CR, the radial velocity dispersion, shown in the bottom panel, at the CR is barely altered after the spiral has died down.

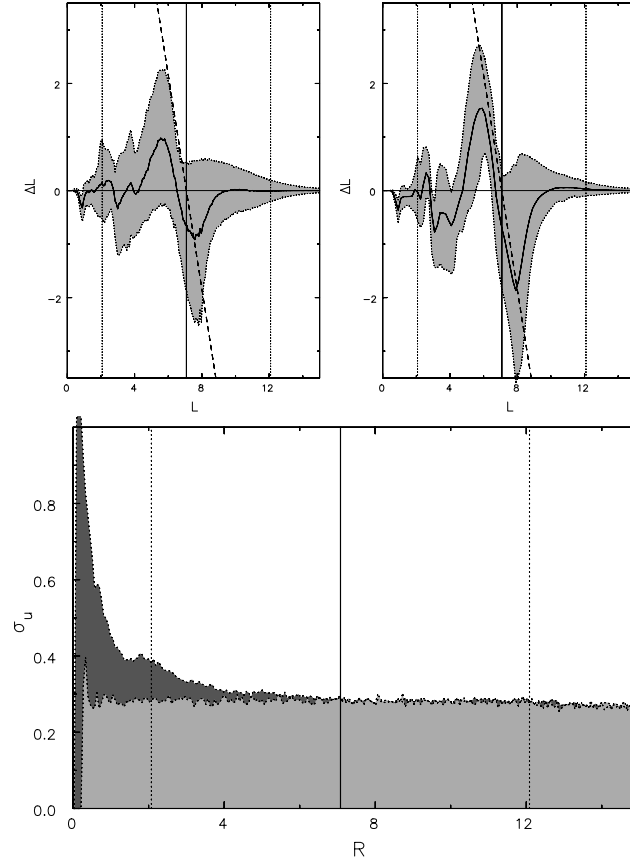


**Fig. 2** *Top*: Exchanges of angular momentum driven by a single spiral. The left panel shows angular momentum exchanges for all orbits while the right panel shows exchanges for nearly circular orbits. The solid vertical line indicates the angular momentum of a circular orbit corotating with the spiral, while the dotted vertical lines show the ILR and OLR. Strong angular momentum exchanges occur at the CR. The shaded region shows the 20% to 80% interval at each angular momentum, with the solid line showing the mean change in angular momentum. *Bottom*: The radial velocity dispersion before (light grey) and after (dark grey) the lifetime of the spiral. The CR (solid line), and the ILR and OLR (dotted lines) are indicated. Although the spiral has driven substantial migration at CR, as shown in the left panels, the radial heating there is negligible. Reproduced with permission from Sellwood and Binney (2002)

A simple way to understand this behaviour is to consider what happens as a spiral density wave forms, increasing the local density in some region. Stars that have  $\Omega > \Omega_p$  will gain energy as they catch up with it, but then lose it again when they overtake

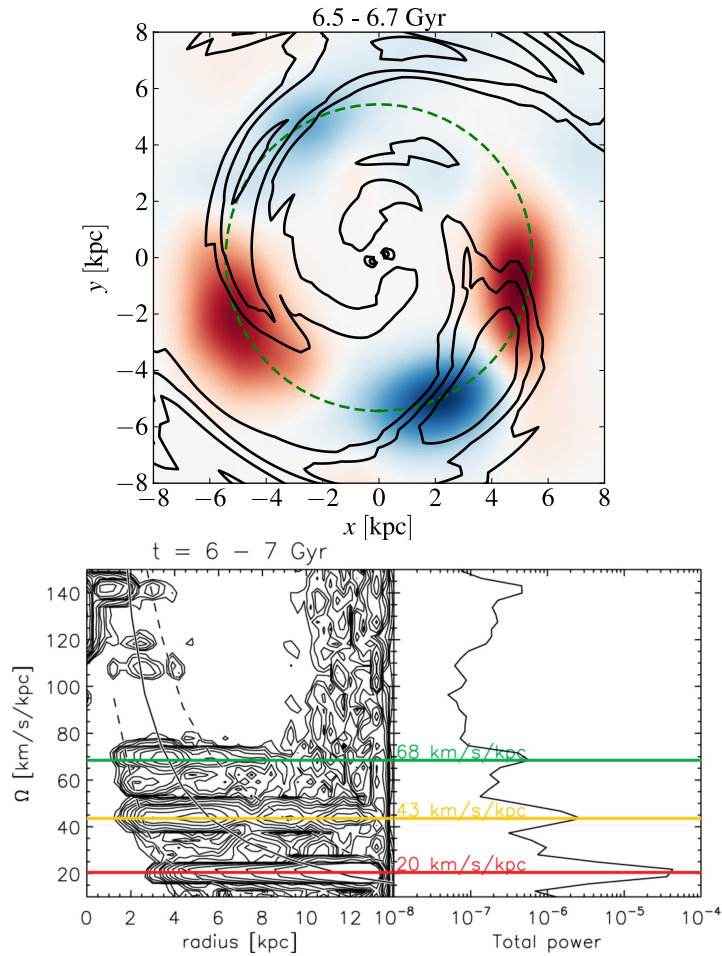


**Fig. 3** *Top*: The location of stars relative to a growing spiral shortly before it reaches peak amplitude, trapping stars and migrating them. The red (blue) shading indicates the density of stars that lose (gain) angular momentum while the contours show the overall density distribution. *Bottom*: The spectrum of spiral structure during the time interval 6–7 Gyr for the same simulation. Three prominent spirals can be seen (with pattern speeds indicated by the horizontal coloured lines) as well as a number of weaker ones. Reproduced with permission from Roškar et al (2012)

it. The net change in energy for such stars is minimal. Conversely the stars with  $\Omega < \Omega_p$  first lose energy, but then gain it again as the spiral overtakes them, also with little net change in energy. Stars that have  $\Omega \simeq \Omega_p$  never overtake, or are overtaken by, the spiral before it decays. These particles are trapped by the spiral, exchanging energy and angular momentum with it. Once the spiral subsides, their net change in angular momentum depends on the relative phase at which they escape. The top panel of Fig. 3 shows the location of stars that are about to be trapped and migrated

by a growing spiral. Stars that will gain angular momentum are located behind the spiral's peak density, while those that will lose angular momentum are ahead of the spiral. The angular phase of the peak density demarcates a separation between the gainers and the losers. Stars are not trapped at just the corotation radius but up to  $\sim 1$  kpc from it. Daniel and Wyse (2015) showed that the trapping region (example shown in Fig. 4) is broadened and not limited to a single radius.

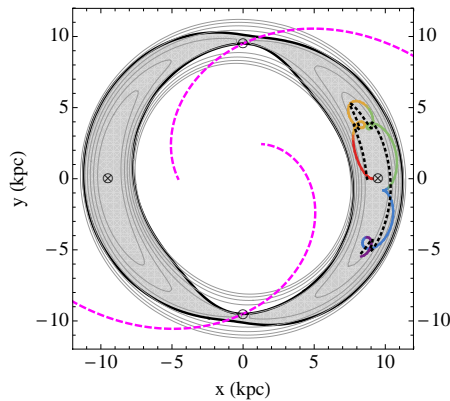


**Fig. 4** Effective potential (grey contours) for a trailing  $m = 2$  spiral, with peak perturbation indicated by dashed magenta lines, having pitch angle  $\theta = 25^\circ$  and CR at 10 kpc. The potential is described in Daniel and Wyse (2015). The crossed circles mark the peak of the effective potential. The capture region is shaded grey. The rainbow path is the trajectory of a trapped star with initial phase-space coordinates  $(x, y, v_x, v_y) = (9.1 \text{ kpc}, 0, 0, -10 \text{ km s}^{-1})$  in the rotating frame. The black (dotted) curve is the star's guiding radius. Figure courtesy of K.J. Daniel

The efficiency of trapping declines rapidly with radial random motion (Sellwood and Binney 2002; Daniel and Wyse 2015; Solway et al 2012), but the vertical random motion reduces the trapping efficiency much more slowly (Solway et al 2012). The left panel of Fig. 5 plots the angular momentum change of stars as a function of orbital eccentricity, showing that angular momentum changes become smaller as the orbital eccentricity increases. The right panel shows that migration is not strongly affected by the vertical amplitude of orbits.

## 3.2 Multiple Patterns

### 3.2.1 Multiple Spirals

Typically disks support multiple spirals with different pattern speeds. The unconstrained simulation of Sellwood and Binney (2002) supported many separate spiral frequencies, which resulted in migration at locations across the disk. Because the difference between initial and final radii of stars was much larger than the epicyclic

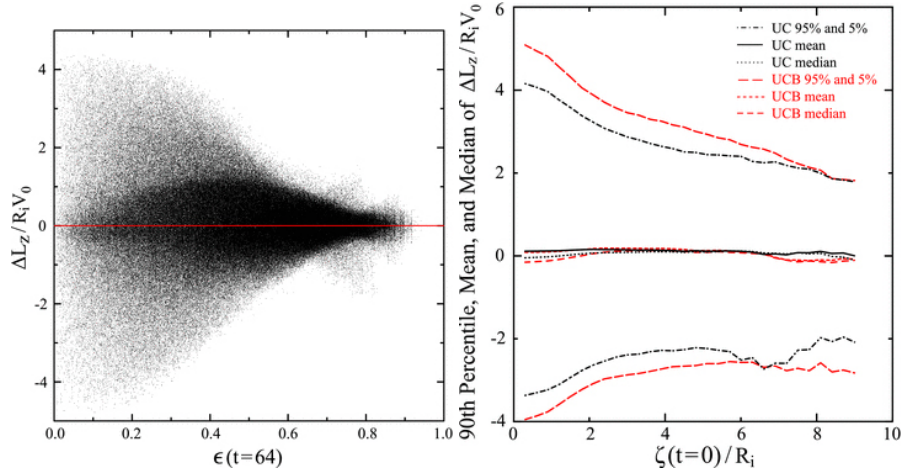


**Fig. 5** *Left*: The effect of orbital eccentricity on migration efficiency. On the horizontal axis is plotted the initial eccentricity of individual stellar orbits, while on the vertical axis is shown the normalised change in angular momentum of the stars. Migration is most efficient for stars on nearly circular orbits. *Right*: The effect of a bar on migration. On the horizontal axis  $\zeta$  is a proxy for the vertical amplitude of the initial orbits. The mean, median and 5% – 95% of the distributions of angular momentum changes are shown by different lines as indicated at top right. Simulation UC (black lines) did not form a bar while simulation UCB, with the same physical model (with  $Q \simeq 1.5$ ) but different random initialisation, formed a bar. The difference is computed over  $\sim 6$  Gyr, during which time a bar formed in UCB within the first Gyr. The effect of the bar on the net migration is small compared to that driven by spirals. Both simulations also show that the effect of height on migration is relatively weak. Reproduced with permission from Solway et al (2012)

radius, particularly at large radii, they concluded that migration by churning was driving this migration. The simulations of Roškar et al (2012) also contained multiple spirals. The bottom panel of Fig. 3 shows a typical example: at least three separate strong spirals with different pattern speeds are clearly recognisable at this particular time. The left panel of Fig. 6 shows the angular momentum exchanges occurring during this time. The presence of multiple spirals increases the number of locations at which stars are migrating (compare with the upper left panel of Fig. 2). For a small, random sample of stars that had large migrations, Roškar et al (2012) showed explicitly that their orbits are trapped by the spiral at the CR.

### 3.2.2 Corotating Spirals

In their simulations, Grand et al (2012) found multiple short spirals such that most of them locally corotate with the stars at a large range of radii. Similar spiral behaviour was also reported by Baba et al (2013) and Roca-Fàbrega et al (2013). Sellwood and Carlberg (2014) demonstrated that this behaviour is a result of several high multiplicity spirals residing in relatively low-mass disks. Grand et al (2012) showed that these spirals trapped a large fraction of the stars at CR, leading to migration

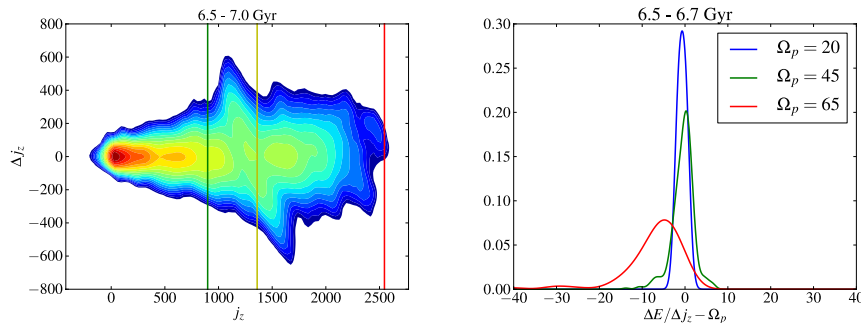


**Fig. 6** *Left*: Distribution of changes in angular momentum as a function of starting angular momentum at around the same time as in Fig. 3. The vertical dashed lines mark the locations of the CR of some of the prominent spirals. *Right*: For stars exchanging angular momentum around each of the main spiral CRs, the distribution of  $\Delta E/\Delta j_z$  is strongly peaked around  $\Omega_p$ . Typical uncertainties on measuring the pattern speeds are  $\sim 5 \text{ km s}^{-1} \text{ kpc}^{-1}$ . Thus the Jacobi energy is a conserved quantity, rather than evolving chaotically, despite the presence of multiple patterns. This implies that large angular momentum exchanges are dominated by the spiral corotation trapping (churning). Reproduced with permission from Roškar et al (2012)

across a large extent of the disk. The extreme migrators in their simulations retain nearly circular orbits, demonstrating that the mechanism is still that of churning.

### 3.2.3 Bars and Chaotic Scattering

The presence of multiple patterns also introduces new physics. Daniel and Wyse (2015) showed that a star trapped at CR can escape if its guiding radius approaches an inner or an outer Lindblad resonance (ILR or OLR) of another pattern, without the spiral amplitude changing. This changes the rate of migration; unlike trapping at the CR, however, this is a scattering process, raising the random motion of stars.

Enhanced migration in the presence of multiple patterns, but especially when a bar is present, has been proposed by a number of studies. Minchev and Famaey (2010) suggested that coupling between multiple patterns (the combination of a bar and spirals, or between multiple spirals) drives strong, chaotic, migration which is substantially more efficient than that driven by churning. The simulations of Minchev et al (2011) exhibited such rapid migration that stellar populations were substantially mixed on a 3 Gyr timescale. Contrary to Debattista et al (2006) and Foyle et al (2008), they suggested that bar-driven migration is persistent. Brunetti et al (2011) also found fast migration (on timescales of order a rotation period) in the case of a bar forming in a cool ( $Q \sim 1$ ) disk, but mixing was much reduced if the initial disk is hot (see also Debattista et al 2006). Halle et al (2015) studied radial redistribution using a bar-unstable simulation, distinguishing between the effects of heating and of churning on the basis of the mean radius of particle orbits. They ar-

gued that the bar’s corotation is the main source of migration. In the outer disk they found heating dominates, rather than migration, by a factor of  $\sim 2 - 8$ .

Other studies have questioned whether such strong migration occurs as a result of multiple patterns. A quantitative assessment of the impact of bars on migration was obtained by Solway et al (2012). The right panel of Fig. 5 compares the degree of angular momentum changes in two models, which represent the same physical initial conditions but, because of the stochasticity inherent in bar formation (Sellwood and Debattista 2009), in one a strong bar formed while in the other no bar formed. The bar formed during the first Gyr; after  $\sim 6$  Gyr of evolution, the change in angular momentum is larger when a bar is present, but not by the order of magnitude predicted by Minchev et al (2011).

Nor is there evidence for strong scattering resulting from the presence of multiple spirals. Roškar et al (2012) tested explicitly for chaotic migration in their simulations with multiple spiral arms (see Fig. 3). They found smoothly evolving orbital frequencies, a characteristic of regular, not chaotic, evolution. Moreover they showed that the changes in energy and angular momentum conserve the Jacobi energy in the frame of the spirals, as shown in the right panel of Fig. 6.  $E_J$  would not be conserved if the chaotic interaction of two or more patterns was scattering the stars, since no stationary closed frame then exists.

The observational evidence also does not favour extremely efficient mixing driven by bars. For instance Sánchez-Blázquez et al (2014) measured stellar age and metallicity gradients in a sample of barred and unbarred galaxies. They found no significant difference in their gradients, arguing that migration by bars is not strong enough to erase gradients.

### 3.2.4 Churning versus Scattering

The word “migration” has come to mean the motion of stars from one radius to another either because of trapping at corotation by spirals (churning) or by a variety of heating mechanisms. As Sellwood and Binney (2002) noted, the measured velocity dispersion of old stars allows very little room for random motions in the Solar neighbourhood to have moved stars by more than  $\Delta R \sim 1.3$  kpc.

*The key difference between churning and scattering is in the random motion created, with churning not increasing random motions appreciably while scattering leads to disks becoming hotter.*

## 3.3 Evidence for Migration in the Milky Way

Because we can study it in much greater detail than other galaxies, thus far the evidence for migration has been strongest in the Milky Way:

- The age-metallicity relation of the Milky Way is flat and broad (Haywood et al 2013; Bergemann et al 2014; Rebassa-Mansergas et al 2016), contrary to the

expected evolution from traditional chemical evolution models. Sellwood and Binney (2002) argued that these are characteristics of migration, as has been shown by models (e.g., Roškar et al 2008a; Schönrich and Binney 2009).

- The radial  $[\text{Fe}/\text{H}]$  gradient decreases with stellar age (Yu et al 2012). Since the metallicity gradient is expected to be steeper at earlier times, this flattening must result from migration smearing the metallicity profile of older stars (Roškar et al 2008a; Schönrich and Binney 2009).
- Bovy et al (2016) showed that low- $[\alpha/\text{Fe}]$ , mono-abundance populations flare radially, which is the expected behaviour for populations that migrate while conserving the vertical action (Solway et al 2012; Vera-Ciro and D’Onghia 2016).
- The skewness of the metallicity distribution function varies across the disk, changing from skewed to low  $[\text{Fe}/\text{H}]$  in the inner disk to skewed to high  $[\text{Fe}/\text{H}]$  at larger radii (Hayden et al 2015). This pattern arises because at larger radii stellar populations include an increasing fraction of metal-rich stars that have migrated outwards from small radii (Hayden et al 2015; Loebman et al 2016).

This partial list demonstrates that a broad range of observations favour migration having occurred in the Milky Way. Whether this is because of churning or scattering is still not decided. The realisation that metal-rich stars, which are probably outward migrators, become proportionally more common at radii past the Solar cylinder hints that the outer disk is a repository of migrated stars.

## 4 Type II Profiles

The type II profile is the most common amongst star-forming galaxies. Two obvious potential causes for a steeper exponential profile in the outer disk are obscuration by dust and a slowly declining star formation rate (SFR). In an  $\text{H}\alpha$  spectroscopic study of 15 edge-on galaxies, Christlein et al (2010) excluded both of these possibilities. Their sample was free of surface brightness enhancements and the data clearly showed a cutoff in the SFR much steeper than that of the stellar continuum. Therefore another mechanism is required to explain the mass in the outer disks.

Pohlen and Trujillo (2006) and Erwin et al (2008) classified type II profiles into various classes based on the break radius and the origin which this suggests. They distinguished between inner and outer breaks, the latter separated into breaks arising from asymmetric disks, classical breaks at large radius and, in barred galaxies, ones at roughly twice the bar radius, which they associated with the bar’s OLR. Pohlen and Trujillo (2006) found classical breaks in 40% of Sc and later-type galaxies.

### 4.1 Theoretical Models

Thus type II breaks are probably due to a number of mechanisms; here we concentrate on classical breaks which are associated with star formation breaks. In the

standard paradigm of galaxy formation, galaxies grow by accreting gas and forming stars (Fall and Efstathiou 1980; Mo et al 1998). Because gas accreted at later times has higher angular momentum, it lands at larger radii (Guo et al 2011). Galaxies should therefore form stars at increasingly large radii, which is termed “inside-out formation”. Inside-out formation predicts that young stars should be present in the outskirts of galaxies (Larson 1976; Matteucci and Franco 1989; Chiappini et al 1997; Naab and Ostriker 2006), as is observed inside the break (de Jong 1996; Bell and de Jong 2000; MacArthur et al 2004; Muñoz-Mateos et al 2007).

#### 4.1.1 Star Formation Breaks

Star formation in disk galaxies typically drops abruptly at a few  $R_d$ , even though the atomic gas extends beyond this point (e.g., Kennicutt 1989; Martin and Kennicutt 2001; Bigiel et al 2010). Efforts to associate stellar breaks with star formation breaks started early (e.g., van der Kruit 1987; Ferguson et al 1998). Schaye (2004) proposed that disk breaks occur as a result of star formation thresholds caused by the phase transition of gas from warm ( $T \sim 10^4$  K) to cold ( $T \sim 10^2$  K). Once this thermal instability sets in, it is quickly followed by a gravitational instability due to the associated sharp drop in Toomre- $Q$ , allowing star formation to proceed. Schaye (2004) computed where the stellar breaks should occur, and found a good match to observed stellar break radii, as shown in Fig. 7. Thus breaks in the stellar distribution show a strong relation to breaks in the present day star formation.

The model of Schaye (2004) assumed that the disk is axisymmetric. Recognising that any perturbations that arise in the outer disk will enhance the local gas density, he predicted that the thermal instability will occur, triggering star formation in the outer disk. Thus it is not surprising to find star formation at large radii, beyond  $2R_{25}$  (e.g., Gil de Paz et al 2005; Thilker et al 2005; Zaritsky and Christlein 2007; Christlein and Zaritsky 2008), with extended UV (XUV) emission in about 20% of galaxies (Lemonias et al 2011), although it is unlikely that all XUV disks can be explained this way. Schaye (2004) also neglected the effects of bars, which are efficient at modifying the distribution of gas. Bars accumulate gas at the OLR (e.g., Schwarz 1981; Byrd et al 1994; Rautiainen and Salo 2000). A bar may also influence the gas further out via resonances of spirals coupled to the bar. Both these effects are present in the barred sample of Muñoz-Mateos et al (2013), who showed that breaks tend to follow two loci (shown in the right panel of Fig. 7): one given by the OLR of the bar, and the other by the OLR of a spiral that has its 4:1 resonance at the CR of the bar. In both cases the effect of bars is to alter the gas distribution and thereby the location of star formation breaks. Finally, star formation need not truncate sharply: Elmegreen and Hunter (2006) proposed a multicomponent star formation model with star formation in the outer disk predominantly driven by turbulent processes (see the review by Elmegreen & Hunter, this volume.)

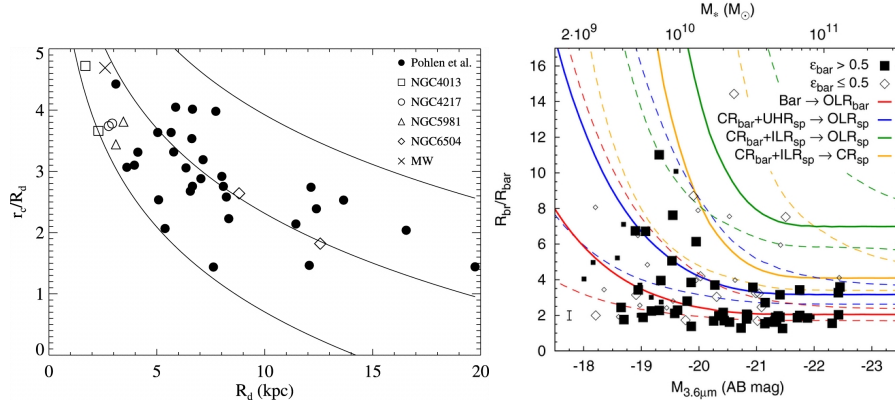


**Fig. 7** *Left*: Break radius,  $r_c$ , as a function of  $R_d$ , in the model of Schaye (2004). The solid lines correspond to disks of different masses ( $M_{\text{disk}} = 7.5 \times 10^9 M_\odot$ ,  $3.8 \times 10^{10} M_\odot$ , and  $1.9 \times 10^{11} M_\odot$ , from top to bottom) assuming a surface density of the phase transition at  $\log(N_{\text{H,crit}} \text{ cm}^{-2}) = 20.75$ . Observational datapoints from the literature are indicated. However, both sides are well fit by models at fixed galaxy mass. Reproduced with permission from Schaye (2004). *Right*: Evidence for the effect of bars on the locations of disk breaks. Filled squares and open diamonds correspond to strong and weak bars. The red solid curve shows the locus of the bar’s OLR while the blue solid line corresponds to the OLR of a spiral which has its inner 4:1 resonance at the bar’s CR. The yellow and green lines are the OLR and CR of spirals with ILR at the bar’s CR. Reproduced with permission from Muñoz-Mateos et al (2013)

#### 4.1.2 Angular Momentum Redistribution Models

Since most stars do not form in the outer disks, stars may reach there from the inner disk. The first mechanism that was proposed to explain type II profiles sought to transform type I profiles via angular momentum redistribution due to coupled bars and spirals (Debattista et al 2006). Their pure  $N$ -body simulations produced spirals with inner 4:1 resonance coinciding with the CR of the bar; angular momentum was transported to the OLR of the spiral, where a break in the profile developed. This angular momentum redistribution occurs *during bar formation*, and decreases thereafter. The left panel of Fig. 8 shows that the break barely evolves after the first 1.5 Gyr, during which time the bar forms. The structural parameters of the resulting breaks are in good agreement with observations, as shown in the right panel of Fig. 8. Debattista et al (2006) found that the inner disk needs to be cool ( $Q \lesssim 1.6$ ) in order for bar formation to require enough angular momentum redistribution to significantly alter the density profile, whereas in hotter disks strong bars formed without a significant break developing. The idea was developed further by Foyle et al (2008), who conducted a large simulation study of bulge+disk systems, including gas and star formation. They found that when breaks form, the outer profile remains unchanged while the inner disk changes substantially. They reported that type II profiles developed when  $m_d/\lambda \geq 1$ , where  $m_d$  is the disk mass fraction and  $\lambda$  is the halo angular momentum. The inclusion of gas led to a break in star formation, but this did not always result in a break in the total profile. In agreement with Debattista

et al (2006), they found that the location of the break does not evolve much once it formed. In a similar spirit, Minchev et al (2011) found that, within 1 – 3 Gyr, as bars form, the density profile of their models extended outwards to more than  $10R_d$ , with a flattened metallicity distribution. Minchev et al (2012) emphasize that outer disks forming via this bar-spiral resonance overlap are radially hot.

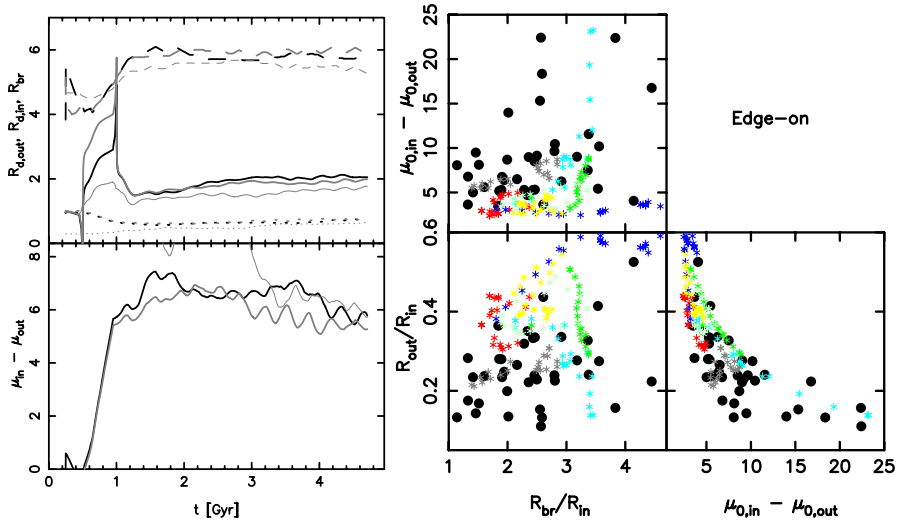


**Fig. 8** *Left:* The evolution of break parameters in the pure  $N$ -body simulations of Debattista et al (2006):  $R_{br}$  (the radius of the break; dashed lines),  $R_{d,in}$  and  $R_{d,out}$  (the scale lengths of the inner and outer disks; solid and dotted lines, respectively), and the difference in central surface brightness between the inner and outer disks,  $\mu_{in} - \mu_{out}$ . In these simulations the bar forms by 1 Gyr. The black, grey and thin lines correspond to different *initial* radial extents of the same model. *Right:* A comparison between parameters of profile breaks in observed (solid circles) and simulated (coloured stars) edge-on galaxies. The observational data are taken from Pohlen (2002). Each simulation corresponds to a different colour and different viewing angles are shown by different points. Reproduced with permission from Debattista et al (2006)

The formation of type II profiles by angular momentum redistribution during bar formation presents a number of difficulties; most obviously strong bars are not present in all galaxies. Minchev et al (2011) argued that bars are a recurrent phenomenon and that the absence of a bar now does not mean that one was never present. However, bars are not easily destroyed (e.g., Shen and Sellwood 2004). Additionally bar destruction leaves a kinematically hot disk; a re-formed bar would subsequently lead to reduced angular momentum transport (Debattista et al 2006; Brunetti et al 2011). The formation of type II profiles in such simulations is likely significantly affected by the very unstable initial conditions usually employed, which may be unlikely in nature.

Another way of scattering material into the outer disk was proposed by Bournaud et al (2007), who used simulations of gas rich disks which form clumps similar to those observed in chain galaxies. These clumps interact gravitationally with each

other, flinging material outwards while sinking to form a central bulge. The material flung out forms a kinematically hot outer exponential of a type II profile. The existence of bulgeless galaxies with type II profiles (e.g., NGC 3589, NGC 6155, UGC 12709; Pohlen and Trujillo 2006) is a challenge for this model to explain type II profiles observed at low redshift since clump formation inevitably also leads to bulge formation.

#### 4.1.3 Churning

Alternatively, Roškar et al (2008b) proposed that the outer disk in type II profiles results from stars that have migrated past the star formation break via churning. Stellar density breaks formed in this way are coincident with a drop in the star formation rate. In their simulations, stars formed from gas continuously cooling from the corona rather than being introduced into the simulation as part of the initial conditions. Because of this, the disk heats as it is forming, remaining at  $Q \simeq 2$  through most of its extent and never becomes violently unstable, while still being cool enough to continuously support multiple spirals. Roškar et al (2008b) found that  $\sim 85\%$  of the stars that end up beyond the break formed interior to it, yet are on nearly circular orbits, with epicyclic radii half of the average radial excursion, which is because spiral trapping is most efficient for nearly-circular orbits.

*In the churning model of type II profiles, while the break radius grows with time, churning forces the break to occur at the same radius for stars of all ages, and all heights above the plane, as seen in Fig. 10. The model also predicts that the mean age of stars beyond the star formation break increases outwards, as shown in Fig. 9. This age upturn occurs because churning, being stochastic, requires increasingly long times to populate regions further from where stars form.*

#### 4.1.4 Insight from Cosmological Simulations

Sánchez-Blázquez et al (2009) studied breaks using a cosmological simulation. The break in the simulation was caused by a drop in the star formation due to a warp, which led to a drop in the volume density of the gas. The stars beyond the break were predominantly (57%) formed interior to the break, with the remainder coming equally from in-situ formation and from satellite accretion. They interpreted the age upturn in their simulation as resulting from a low but constant star formation at large radii, rather than to migration. Ruiz-Lara et al (2016a) also found age upturns in their cosmological simulations, which were caused by satellites accreted onto the outer disks. An observational signature of such accretion is that past the break the age upturn is followed within  $\sim 1 R_d$  by an age plateau.

However, cosmological simulations are still plagued by excessively hot disks. Sánchez-Blázquez et al (2009) dealt with this by identifying the disk component via a kinematic cut on stellar orbits to retain stars on nearly circular orbits. This resulted in a meagre 37% of stars being sufficiently cool to be considered as disk stars.

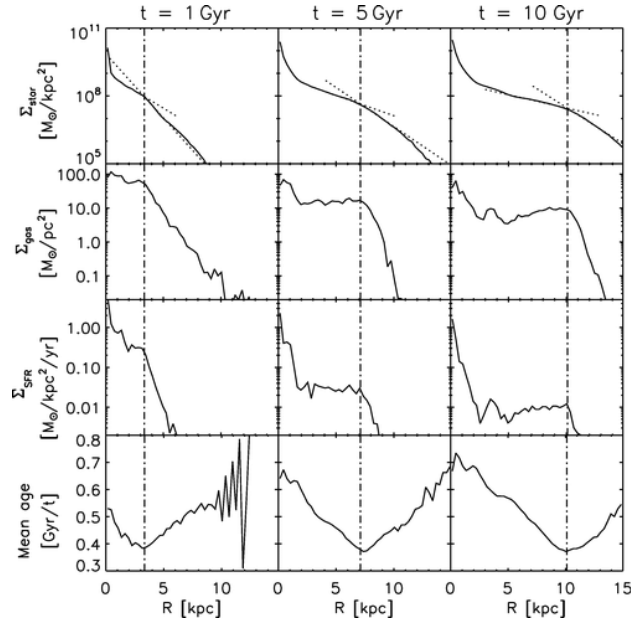


**Fig. 9** Evolution of the system with stars forming from gas cooling off a hot corona. The *top* row shows the stellar density profile, the *second* row shows the surface density of cool gas, the *third* row shows the star formation rate surface density and the *bottom* row shows the average age of stars, normalised to the age of the galaxy at that time. From *left* to *right* the columns show the system after 1, 5, and 10 Gyr. The vertical dot-dashed lines show the stellar break radius while the dotted lines in the top row show the inner and outer exponential disk fits

Likewise Ruiz-Lara et al (2016a) applied a kinematic cut to the stellar particles, but were left with a hot system with even young populations being as hot as the old stars in the Solar neighbourhood. Roškar et al (2010) stressed that however the disk is defined, one is left with a high Toomre- $Q$  system which substantially inhibits spiral structure (e.g., Binney and Tremaine 2008), suppressing churning; therefore these simulations cannot yet give a clear indication of the relative contribution of accreted, scattered and migrated by churning stars in outer disks.

## 4.2 Observational Tests

### 4.2.1 Resolved Stellar Population Studies

Resolved stellar population studies are ideal for assessing the populations of outer disks because they can be observed directly and little modelling is necessary. An early study of stellar populations across the break came from the GHOSTS survey (Radburn-Smith et al 2011) for the edge-on galaxy NGC 4244 (de Jong et al

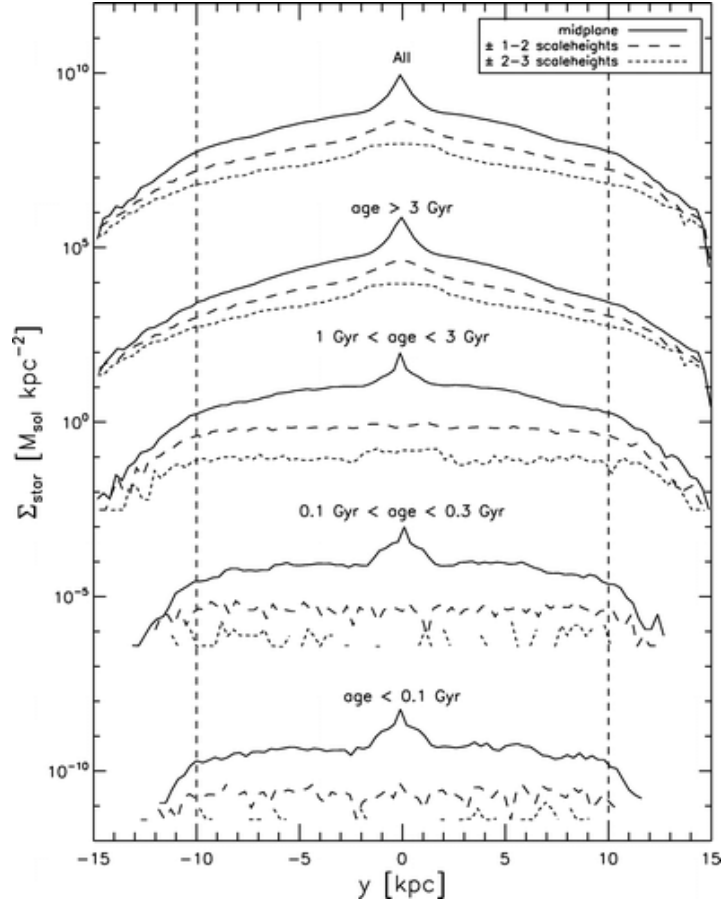


**Fig. 10** The density distribution of stars for the galaxy on the left at 10 Gyr, observed edge-on. Different age bins are shown, as indicated, with the top profiles showing the profiles of all the stars. In each set of profiles, three heights above the mid-plane are shown, as indicated in the inset. An arbitrary offset has been applied to each set of profiles, for clarity. Reproduced with permission from Roškar et al (2008b)

2007). They separated stars into four age bins at different heights above the mid-plane. They found that stars of all ages have a break at the same radius, regardless of whether they are in the mid-plane or above it, as seen in Fig. 11. Unless the break formed very recently (for no apparent reason), or formed once and has not evolved since (whereas observations show that break radii have evolved since  $z \sim 1$ , e.g., Pérez 2004; Trujillo and Pohlen 2005; Azzollini et al 2008b) the most plausible explanation is that the break radius evolves with time, with something forcing all stars to adopt a common break radius. The churning model predicts exactly this behaviour: as seen in Fig. 9, the break radius in the simulations of Roškar et al (2008b) evolves with time, yet the location of the break is identical for all populations.

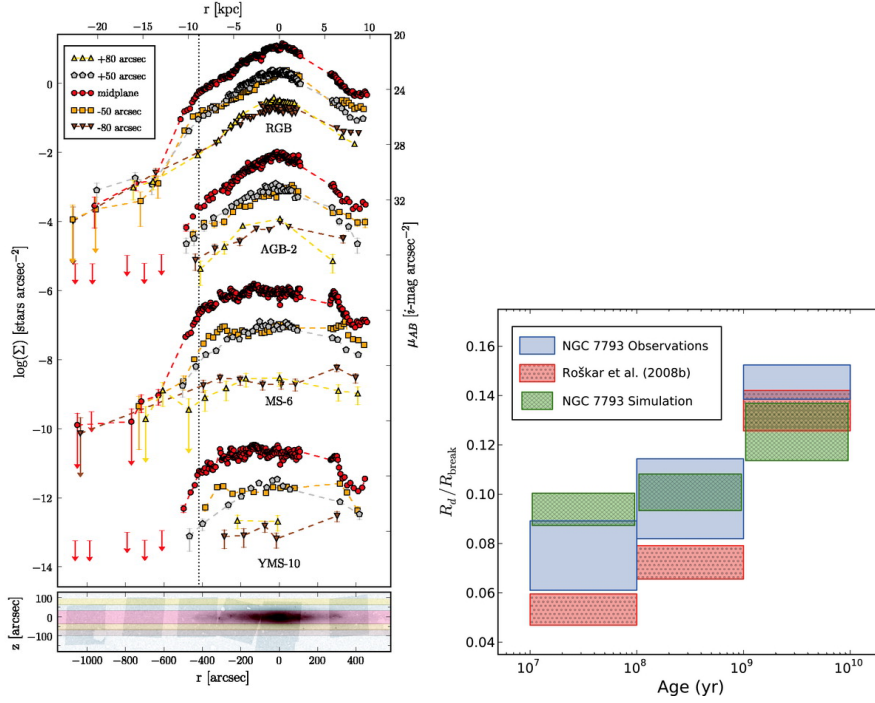


**Fig. 11** *Left*: Radial density profiles for resolved stellar populations in the edge-on NGC 4244 (shown at bottom). The different populations are young main sequence (YMS) stars ( $< 100$  Myr), main sequence (MS) stars ( $100 - 300$  Myr), asymptotic giant branch (AGB) stars, (older than  $0.3$  Gyr and peaking at  $1 - 3$  Gyr with a tail to  $10$  Gyr) and metal poor red giant branch (RGB) stars (older than  $5$  Gyr). Five strips are used, as indicated at top-left, at three different offsets from the mid-plane. The AGB, MS and YMS profiles have been offset vertically by  $-2$ ,  $-6$  and  $-10$  respectively, for clarity. This can be compared with Fig. 10. Reproduced with permission from de Jong et al (2007). *Right*: The outer disk exponential scale lengths, normalised by the break radius, as a function of age for NGC 7793 (shaded blue box) and two simulations: the Milky-Way mass one of Roškar et al (2008a) (dotted red box) and another of the same mass and size as NGC 7793 (hatched green box). The height of the boxes represents the uncertainty on the scale-length. Reproduced with permission from Radburn-Smith et al (2012)

A second example of a type II profile with a common break radius for all ages is the low-inclination flocculent spiral galaxy NGC 7793 (Radburn-Smith et al 2012). Here, the break is just inside the break of both the HI gas, and of the star formation. Beyond the break  $R_d$  increases with the age of the stellar population. Fig. 11 shows the scale-length of different age bins for NGC 7793, and for a simulation of a galaxy of comparable mass and size which experienced significant churning.

M33 also has a type II profile with a break at  $\sim 8$  kpc (Ferguson et al 2007), which is present also in the surface mass density (Barker et al 2011); stars past the break exhibit a positive age gradient (Barker et al 2007; Williams et al 2009; Barker et al 2011). Unlike NGC 4244 and NGC 7793, M33 has had a strong interaction,

in the past 1 – 3 Gyr (Braun and Thilker 2004; Putman et al 2009; Davidge and Puzia 2011). Barker et al (2011) found that about half of all stars just inside the break have ages between 2.5 Gyr and 4.5 Gyr, with less than 14% of stars older. While the star formation within 8 kpc does not appear to have changed much in the past few Myr, the main sequence luminosity function of the outer disk indicates that the recent star formation rate in the outer disk has declined (Davidge and Puzia 2011), suggesting enhanced star formation in the outer disk or contamination by young stars. In the past 10 Gyr  $R_d$  has increased by a factor of  $\sim 2$ . Williams et al (2013) contrasted M33 with its near equals in mass, NGC 300 and NGC 2403, both relatively isolated bulgeless late-type galaxies with type I profiles. They concluded that the environment has played a role in the formation of the break in M33.

#### 4.2.2 Spectroscopic Studies

Yoachim et al (2012) modelled integral field data for six type II profile galaxies, obtaining their star formation history. In all cases the average age profile has a positive gradient beyond the break. The modelling fitted an exponentially declining SFR,  $\psi(t) \propto e^{-t/\tau}$ , where the time-scale,  $\tau$ , was allowed to take both positive (declining SFR) and negative (increasing SFR) values. In three of the six galaxies,  $\tau$  was positive, as expected if the stars in this region migrated there. The other three galaxies had negative  $\tau$ , indicating an increasing SFR, which is not expected if the outer disk formed exclusively from migrated stars. Fig. 12 presents an example of each behaviour. NGC 6155, shown on the right, is a galaxy where the stellar populations past the break have a radially increasing average age and, except for the innermost bin, temporally decreasing star formation rate. While the average stellar age increases past the break, the minimum age is not at the break itself, but half way between the centre and the break; inspection of the top panel of Fig. 12 shows that, at the location of the age minimum, the galaxy has a strongly star-forming ring encircling a bar.

*Churning predicts that the mean age increases past the break. However, the break need not be the location of the minimum in average age, which happens only if inside-out growth is exact.*

Another example of an age minimum before the break radius is M95, a barred galaxy with a ring at  $\sim 8$  kpc previously classified as having an OLR type II profile (Erwin et al 2008). However, the star formation break is at  $\sim 13$  kpc, beyond which the colour gradient reverses, extending to  $\sim 25$  kpc (Watkins et al 2014).

For three galaxies, Yoachim et al (2012) found that the star formation timescale remains negative (increasing SFR) to the last measured point. The left panels of Fig. 12 show an example, IC 1132. What appears to be happening in each of these galaxies is that new stars are forming in-situ due to spirals extending past the break radius, as envisaged by Schaye (2004). Since the SFR does not terminate at the break, either in the observations or in the simulations (Roškar et al 2008b found that 15% of stars formed in-situ), it should not be surprising to find hints of recent

star formation past the break. Moreover, such galaxies are easier to measure spectroscopically so may be over-represented in a small sample.

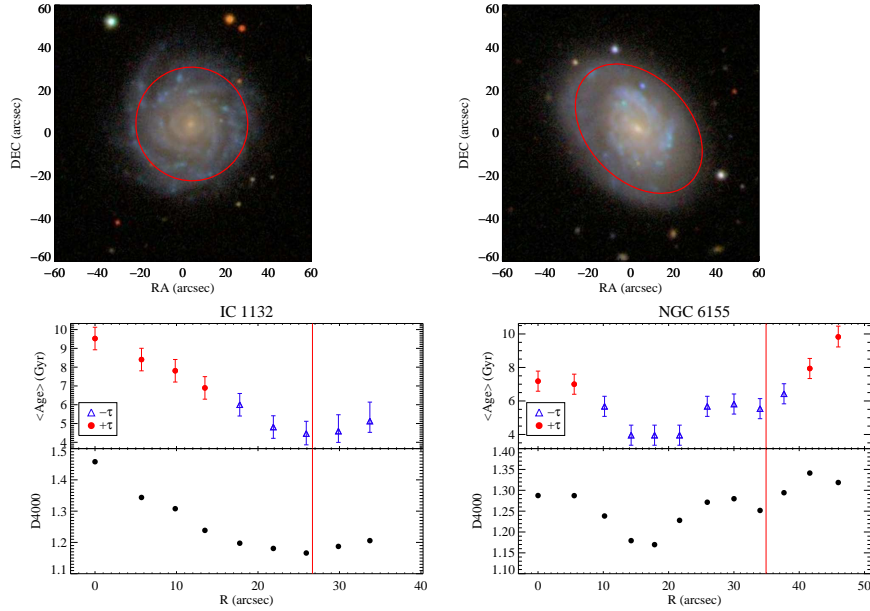


**Fig. 12** *Left:* IC 1132. *Right:* NGC 6155. The *top* row shows images of the galaxies with the location of the break indicated by the red ellipses. The *bottom* row shows the mean age profiles (top panel) and the D4000 index (*bottom* panel). In the mean age profiles, blue points correspond to  $\tau < 0$  (exponentially increasing SFR), while the red points correspond to  $\tau > 0$  (exponentially decreasing SFR). Reproduced with permission from Yoachim et al (2012)

Ruiz-Lara et al (2016b) studied the stellar populations of 44 face-on spiral galaxies from the CALIFA survey. They found that  $\sim 40\%$  of these show age upturns beyond the break in the luminosity-weighted spectra. They found very flat mass-weighted mean age profiles, with less than 1 Gyr variation in NGC 551 and NGC 4711. Moreover, they found that luminosity-weighted mean age upturns are present in both type II and type I profiles. Roediger et al (2012) had also seen age upturns in type I profiles for galaxies in the Virgo Cluster. This suggests that age upturns in type I galaxies may be a result of environment (see Sect. 5 below). Their presence in type I profiles led Ruiz-Lara et al (2016b) to propose that age upturns are the result of the early formation of the entire disk followed by a gradual inside-out quenching of star formation.

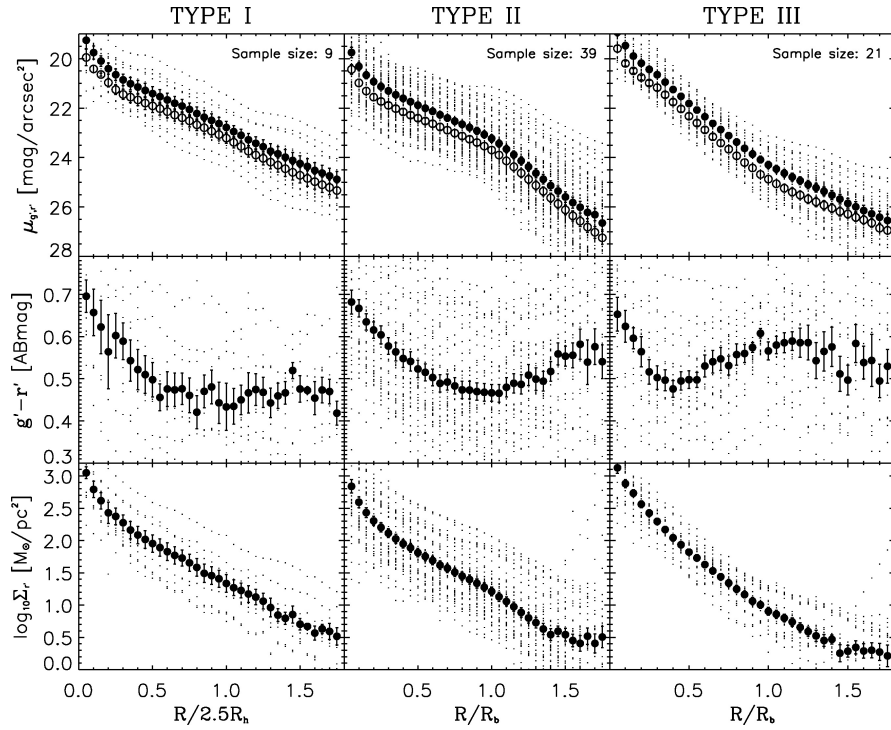


**Fig. 13** Stacked profiles of 9 type I (*left*), 39 type II (*middle*) and 21 type III (*right*) galaxies. The *top* row shows the  $r'$  (filled circles) and  $g'$  profiles (open circles). The *middle* row shows the  $g' - r'$  colour profiles. The *bottom* row shows the computed mass density profiles. Reproduced with permission from Bakos et al (2008)

### 4.2.3 Photometric Methods

Because of the age-metallicity degeneracy (e.g., Worthey 1994), colour profiles are less constraining in probing the stellar populations of outer disks. Azzollini et al (2008a) stacked colour (approximating rest-frame  $u - g$ ) profiles of different profile types to  $z \sim 1.1$ . They scaled the radius by the break radius in type II and III galaxies and to  $2R_d$  in type I galaxies. In the type I galaxies, the resulting colour profiles are flat or slightly rising, with no features. Likewise the type III galaxies showed a range of gradients ranging from negative to positive with increasing redshift. Type II galaxies instead become increasingly red past the break at all redshifts. For a sample of nearby late-type galaxies, Bakos et al (2008) carried out a similar stacking analysis, shown in Fig. 13; they used the colour profiles to obtain mass-to-light ratios, and thereby recovered the mass profiles. They found that galaxies with type II profiles have much weaker breaks in the overall *mass* distribution than in the light. Zheng et al (2015) stacked a larger sample of 698 galaxies spanning a wide range of mass and morphology. In the bluer bands, in the majority of galaxies they found type II profiles, becoming type I in red bands, in contradiction to Martín-Navarro

et al (2012), who found numerous examples of type II profiles in red bands, albeit weaker than in the blue. However, the latter authors stacked galaxies at fixed  $r_{90}$  rather than to the break radius, which probably smears any weak breaks.

### 4.3 Synthesis and Outlook

Evidence that the outer disks of type II profiles are due to migration comes from the increasing age of stars past the break; in contrast an outer disk dominated by accretion would have a constant age profile. The coincidence of star formation breaks and stellar continuum breaks, and the common break for stars of all ages, favours the churning model. However, the evidence is not yet conclusive. Measurements of kinematics in the outer disks would provide definitive proof of whether migration is dominated by scattering or by churning. Further observational study and modelling of the role of environment is also required. The extent to which the mass profile deviates from pure exponential needs further study and may help constrain the relative importance of churning and scattering.

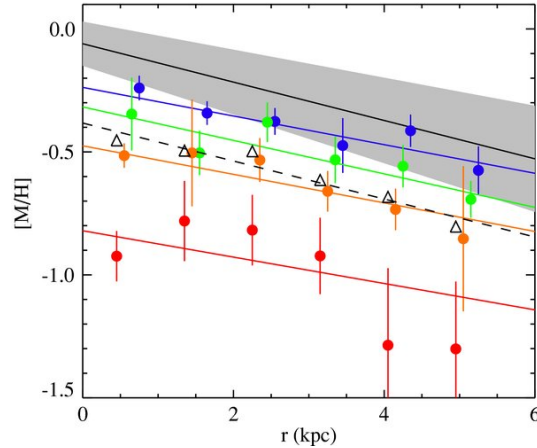
## 5 Type I Profiles

Type I profiles, extending to  $\sim 6 - 8 R_d$ , are present in roughly 10% – 15% of field late-type spirals (Gutiérrez et al 2011). Examples of galaxies with type I profiles are sufficiently nearby that their stellar populations can be resolved and studied directly. NGC 300 is a relatively isolated, unbarred galaxy with a type I profile extending unbroken to 10 disk scale-lengths ( $\sim 14$  kpc; Bland-Hawthorn et al 2005). Using *HST* to resolve the stellar populations of the inner  $\sim 5$  kpc, Gogarten et al (2010) showed that the majority of its stars are old (see also Vlajić et al 2009), with 80% of them older than 6 Gyr.  $R_d$  increases from 1.1 kpc for old stars to 1.3 kpc for young stars, indicating a modest inside-out formation, which is also evident in the broad-band colours (Muñoz-Mateos et al 2007). Bland-Hawthorn et al (2005) estimated that everywhere beyond  $\sim 6$  kpc the Toomre- $Q = 5 \pm 2$ . Thus spiral structure in NGC 300 is unlikely to be strong, which, together with its low surface mass density, makes churning inefficient, as confirmed by simulations (Gogarten et al 2010). In agreement with this prediction, both young stars (Kudritzki et al 2008) and old stars (Vlajić et al 2009; Gogarten et al 2010) exhibit the same negative metallicity gradient outside 2 kpc, which has remained quite constant over the past  $\sim 10$  Gyr (Gogarten et al 2010), as seen in Fig. 14.

NGC 300 is not unique: NGC 2403 is another nearby, isolated bulgeless galaxy with a type I profile. Whereas NGC 300 has a strong HI warp, NGC 2403 has no warp (Williams et al 2013). All stellar populations, including the young stars, follow the same density profile, with no break. The star formation histories are parallel at

all radii to  $11R_d$ , with the surface density of star formation following the same exponential profile as the overall density profile (Williams et al 2013).

**Fig. 14** The metallicity profiles of NGC 300. Solid black line with grey shaded region: metallicity profile of 24 young A-type supergiants from Kudritzki et al (2008). Blue, green, orange and red circles are the metallicity profiles for stars with ages  $< 100$  Myr, 1 – 5 Gyr, 5 – 10 Gyr, and 10 – 14 Gyr, respectively. The black triangles and dashed line indicate the mean metallicity for the entire population. Reproduced with permission from Gogarten et al (2010)



### 5.1 Origin of Type I Profiles in Isolated Galaxies

These observational results help constrain the origin of type I profiles. Minchev et al (2011) proposed that the type I profile of NGC 300 was produced by very efficient migration driven by resonance overlap scattering. The presence of the radial metallicity gradients, which have remained almost constant over  $\sim 10$  Gyr, severely limits the possibility that such migration has occurred in NGC 300. The fact that its stars are predominantly old means that migration would have had ample time to flatten any metallicity gradient if it had been important. The low mass and large Toomre- $Q$  of the disk make it an unlikely candidate for strong spiral structure, making extreme migration even less likely to have occurred. The large Toomre- $Q$  could have been produced by a bar heating the disk, but NGC 300 is bulgeless, whereas angular momentum redistribution by a bar would have produced a bulge-like central mass concentration (Debattista et al 2006). A similar case can be made for NGC 2403.

Herpich et al (2015a) proposed that the shapes of density profiles depend on the angular momentum of the gas corona out of which the disk forms. At low spin parameter,  $\lambda$ , their simulations formed type III profiles (see below) while at high  $\lambda$  they formed galaxies with type II profiles. For galaxies with an intermediate angular momentum ( $0.035 \leq \lambda \leq 0.04$ ) they formed type I profiles. This model very naturally accounts for the relative rarity of the type I profile. Furthermore, because it does not require stars to migrate, this model is consistent with the metallicity gradients in NGC 300 and in NGC 2403. The absence of a break in the profiles of stars younger than 200 Myr in NGC 300 also supports this model. Lastly, this scenario is

also consistent with the fact that the *inner* profiles of type II and type I galaxies are consistent with each other (Gutiérrez et al 2011).

## 5.2 Type I Profiles in Cluster Lenticulars

While type I profiles are rare in the field, they are common amongst cluster lenticulars (see Sect. 2.1). Since a narrow range of  $\lambda$ s cannot account for a dominant population, a different explanation for type I profiles in cluster lenticulars is required. Clarke et al (2017) evolved the model of Roškar et al (2008b) (with  $\lambda = 0.065$ ) in a cluster environment. Their model galaxy was quenched by ram pressure stripping and transformed into a lenticular with very little spiral structure at late times. At the time of peak ram pressure stripping, the disk had a break radius at  $\sim 6$  kpc; therefore the galaxy never gets a chance to form many stars beyond this radius. As shown in Fig. 9, the same model evolved in isolation resulted in a type II profile with a break at 10 kpc. Nonetheless stars in the cluster galaxy moved to large radii through migration via strong, tidally-induced, spirals, but not through heating of the disk. As a result, a type I density profile developed, as shown by the top panel of Fig. 15. This combination of quenching by ram pressure stripping, and churning by tidally-induced spirals accounts for the high incidence of type I profiles amongst cluster lenticulars. Because of the strong churning into the outer disk, Clarke et al (2017) predicted that the age profile of cluster lenticulars with type I profiles will be flat or slightly rising past the point where the galaxy had a break radius before star formation is quenched, as shown in the bottom panel of Fig. 15. Indeed for the Virgo Cluster, Roediger et al (2012) used colour profiles to show that more than 70% of galaxies with type I profiles have flat or slightly positive age gradients.

## 6 Type III Profiles

Erwin et al (2005) identified two kinds of type III profiles. The first kind is produced by the excess light above an exponential from a stellar halo. They argued that such galaxies can be recognised by their outer isophotes becoming rounder. M64 is an example of such a galaxy (Gutiérrez et al 2011); its outer profile is well fit by a power law, typical of a halo. The presence of counter-rotating gas, with star formation concentrated within the inner 4.5 kpc, attests to M64 being a post-merger galaxy (Watkins et al 2016), which probably produced the prominent halo. In such cases, Martín-Navarro et al (2014) showed that the halo may mask the presence of an underlying type II profile in the disk, particularly at low inclination. Erwin et al (2005) estimated that haloes account for  $\sim 30\%$  of their sample of type III profiles.

In the majority of their type III galaxies, however, Erwin et al (2005) found sharp transitions from one exponential to a shallower one, with isophotes not becoming significantly rounder and, in some cases, hosting spiral arms. Maltby et al (2012b)

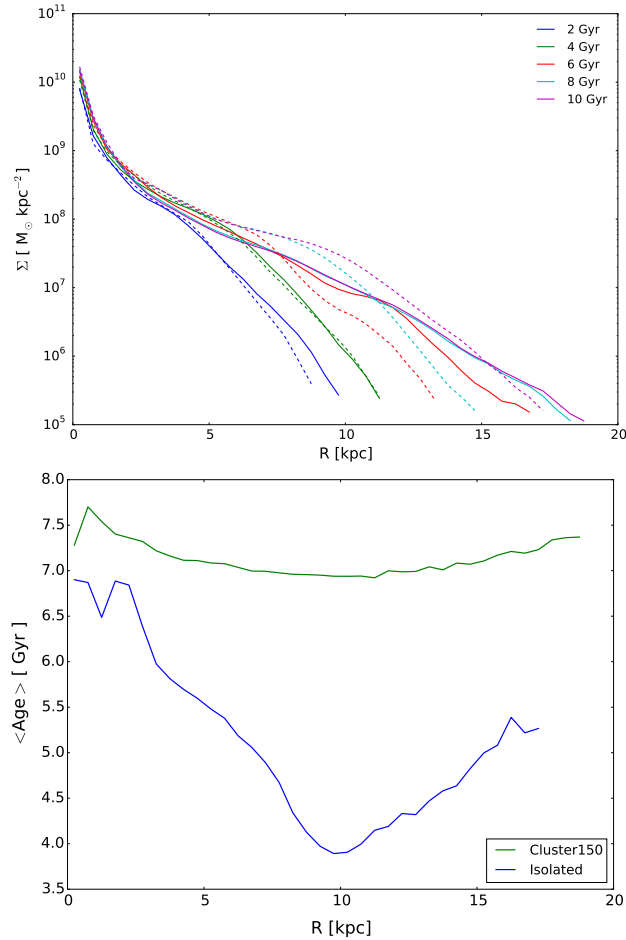


**Fig. 15** *Top*: Evolution of surface density profile of the model of Roškar et al (2008b), when evolved in isolation (dashed lines) and when it falls into a cluster, reaching pericentre at 5 Gyr (solid lines). Whereas the isolated simulation develops a type II profile, the same system evolving in the cluster is transformed into a type I profile via the joint action of ram pressure stripping and tidally-induced spirals. *Bottom*: The final mean age profiles of the isolated and cluster models. The isolated model has an increasing average age past the break, whereas the cluster model has a nearly flat age distribution. Reproduced with permission from Clarke et al (2017)

showed that in  $\sim 85\%$  of cases the extrapolation of the bulge profile to large radii is insufficient to account for the excess light at the break. Thus, except in cases where the light profile is flattened by the point spread function (see the review by Knapen & Trujillo, this volume), the majority of type III profiles are a disk phenomenon.

## 6.1 Formation of Type III Disk Profiles

Breaks in type III profile galaxies are not associated with a colour change (Azzollini et al 2008a; Bakos et al 2008; Zheng et al 2015). Changes in stellar populations and star formation are therefore not the origin of these profiles.

Anecdotally, Erwin et al (2005) noted that a number of galaxies with type III profiles exhibit asymmetries in the outer disks while Pohlen and Trujillo (2006) found evidence of recent interactions amongst type III galaxies. It is unsurprising therefore that many models of type III profile formation rely on mergers and interactions. Laurikainen and Salo (2001) used simulations to show that interactions result in long-lasting shallow outer profiles. Peñarrubia et al (2006) proposed that extended outer disks are composed of tidally disrupted dwarf satellites accreted directly onto the plane of the disk. They showed that the degree of rotational support of the accreted material depends on the satellite orbit, with dispersion increasing with orbital eccentricity. Instead of the outer disk being accreted, Younger et al (2007) proposed that it forms from the main disk itself after a minor merger forces gas to the centre, causing the galaxy's inner region to contract and its outer region to expand. In the absence of gas, the pure  $N$ -body simulations of Kazantzidis et al (2009) produced type III profiles when substructures excited angular momentum redistribution within the disk. Borlaff et al (2014) demonstrated that, in simulations, gas-rich major mergers, which destroy the main disk then build a new one at large radius, develop into S0 galaxies with type III profiles.

Alternatively both Minchev et al (2012) and Herpich et al (2015b) proposed that type III profiles formed via the action of bars. Minchev et al (2012) invoke resonance overlap in the presence of a bar together with gas accretion to populate the outer disk. In the model of Herpich et al (2015b), instead, stars in the inner disk gained energy directly from the bar, getting boosted to increasingly eccentric orbits, and reaching large radii.

Observations do not yet provide very strong constraints on how type III profiles form. The lack of an observed difference between type III profiles in barred and unbarred galaxies (Borlaff et al 2014; Eliche-Moral et al 2015), and the fact that type III profiles are *less* common amongst barred galaxies in the field (see Table 1) suggests that bars are unlikely to account for the majority of type III profiles. In edge-on galaxies, anti-truncations appear in thick disks, supporting the view that a hot population is responsible for the outer disk (Comerón et al 2012), contrary to the model of Borlaff et al (2014). The most promising models therefore are the direct accretion model (Peñarrubia et al 2006) and the heating by substructure model (Kazantzidis et al 2009), both of which produce hot outer disks. The model of Younger et al (2007) may also lead to hot outer disks because of the rapid change of the inner potential. Which of these models works best can be decided by measuring the kinematics of both inner and outer disks, as well as the chemistry of the outer disk. Additional constraints may be possible from comparing the properties of type III and type I/II. For instance, Gutiérrez et al (2011) note that the inner exponentials of type III galaxies have shorter scale-lengths and higher central sur-

face brightness than galaxies with type I profiles, which argues against the direct accretion model but might favour the model of Younger et al (2007).

## 7 Future Prospects

Much work remains to be done to better distinguish between competing scenarios of outer disk formation, and to clarify what role, if any, migration has played. With the imminent launch of the *JWST*, resolved stellar population studies will be possible in a volume roughly three times larger than is accessible with *HST*, improving the statistical robustness of age and metallicity dissections of outer disks. In addition, we identify three areas that would greatly advance our understanding of disk outskirts.

- *Kinematics in the outer disks in type II galaxies* The two classes of models for producing the outer disks of type II profiles make very different kinematic predictions. Models based on scattering of stars from the inner disk all produce radially hot outer disks. In contrast, churning predicts a relatively cooler outer disk. The observed line-of-sight velocity dispersion,  $\sigma_{\text{los}}$ , is given by

$$\sigma_{\text{los}}^2 = \frac{1}{2} \sin^2 i [(\sigma_{\text{R}}^2 + \sigma_{\phi}^2 + 2\sigma_z^2 \cot^2 i) - (\sigma_{\text{R}}^2 - \sigma_{\phi}^2) \cos 2\phi], \quad (3)$$

where  $\sigma_{\text{R}}$ ,  $\sigma_{\phi}$ , and  $\sigma_z$  are the velocity dispersions in the radial, tangential and vertical directions, respectively,  $i$  is the galaxy's inclination and  $\phi$  is the angle from the major axis of the disk in its intrinsic plane. This can be written as  $\sigma_{\text{los}}^2 = a(R) + b(R) \cos 2\phi$ . The first term,  $a(R)$ , is positive definite and independent of  $\phi$ . The second term,  $b(R)$  is proportional to  $-\beta_{\phi} = -(1 - \sigma_{\phi}^2/\sigma_{\text{R}}^2)$ ; it is therefore negative in the inner disk where generally  $\beta_{\phi} > 0$ . When the outer disk is formed of material that migrated via churning, then it is kinematically relatively cool and  $b(R)$  remains negative. If instead the outer disk is comprised of stars scattered outwards, then  $\beta_{\phi} < 0$  and  $b(R)$  is positive. In the former case,  $\sigma_{\text{los}}$  peaks on the major axis, while it peaks on the minor axis for scattering. This provides a very promising means for distinguishing which class of models is responsible for the outer disks in type II galaxies.

- *Kinematics of type III galaxies* Most models of type III galaxies predict that outer disks, and, for some models, the inner disk, are hot, and that the outer disk is comprised of stars that have been moved out, or accreted directly. Confirming this prediction would give us an important insight into the properties of galaxies that have experienced these heating or accretion processes.
- *The outer disk of the Milky Way* As with many other aspects of galaxy evolution, the Milky Way provides an important laboratory for our understanding of disk outskirts. In the era of *Gaia* we should be able to study the ages, metallicities, abundances and 3-D kinematics of stars past the break. This will allow us to test the relations between the outer disk and the inner disk, the warp, and the

bar. Accreted stars may also be identified. These data will result in a much more detailed picture of the origin of the Milky Way's outer disk.

While the field of disk outskirts has made huge strides in the past decade, the next decade promises to be even more exciting in terms of understanding their assembly. Confirmation of an important role for radial migration would permit an important means for assessing its *overall* action on disk galaxies.

## 8 Acknowledgements

VPD is supported by STFC Consolidated Grant #ST/M000877/1. We thank Kathryn Daniel for providing us with the unpublished Figure 4. Discussions with Peter Erwin have been especially enlightening. VPD thanks the Max-Planck-Institut für Astronomie for hosting him during which time this review was started.

## References

- Azzollini R, Trujillo I, Beckman JE (2008a) Color Profiles of Disk Galaxies since  $z \sim 1$ : Probing Outer Disk Formation Scenarios. *ApJ*679:L69–L72, DOI 10.1086/589283, [arXiv:0804.2336](https://arxiv.org/abs/0804.2336)
- Azzollini R, Trujillo I, Beckman JE (2008b) Cosmic Evolution of Stellar Disk Truncations: From  $z \sim 1$  to the Local Universe. *ApJ*684:1026–1047, DOI 10.1086/590142, 0805.2259
- Baba J, Saitoh TR, Wada K (2013) Dynamics of Non-steady Spiral Arms in Disk Galaxies. *ApJ*763:46, DOI 10.1088/0004-637X/763/1/46, 1211.5401
- Bakos J, Trujillo I, Pohlen M (2008) Color Profiles of Spiral Galaxies: Clues on Outer-Disk Formation Scenarios. *ApJ*683:L103, DOI 10.1086/591671, 0807.2776
- Barker MK, Sarajedini A, Geisler D, Harding P, Schommer R (2007) The Stellar Populations in the Outer Regions of M33. III. Star Formation History. *AJ*133:1138–1160, DOI 10.1086/511186, [astro-ph/0611892](https://arxiv.org/abs/astro-ph/0611892)
- Barker MK, Ferguson AMN, Cole AA, Ibata R, Irwin M, Lewis GF, Smecker-Hane TA, Tanvir NR (2011) The star formation history in the far outer disc of M33. *MNRAS*410:504–516, DOI 10.1111/j.1365-2966.2010.17458.x, 1008.0760
- Bell EF, de Jong RS (2000) The stellar populations of spiral galaxies. *MNRAS*312:497–520, DOI 10.1046/j.1365-8711.2000.03138.x, [astro-ph/9909402](https://arxiv.org/abs/astro-ph/9909402)
- Bergemann M, Ruchti GR, Serenelli A, Feltzing S, Alves-Brito A, Asplund M, Bensby T, Gruyters P, Heiter U, Hourihane A, Korn A, Lind K, Marino A, Jofre P, Nordlander T, Ryde N, Worley CC, Gilmore G, Randich S, Ferguson AMN, Jeffries RD, Micela G, Negueruela I, Prusti T, Rix HW, Vallenari A, Alfaro EJ,

- Allende Prieto C, Bragaglia A, Koposov SE, Lanzafame AC, Pancino E, Recio-Blanco A, Smiljanic R, Walton N, Costado MT, Franciosini E, Hill V, Lardo C, de Laverny P, Magrini L, Maiorca E, Masseron T, Morbidelli L, Sacco G, Kor-dopatis G, Tautvaišiene G (2014) The Gaia-ESO Survey: radial metallicity gradients and age-metallicity relation of stars in the Milky Way disk. *A&A*565:A89, DOI 10.1051/0004-6361/201423456, 1401.4437
- Bigiel F, Leroy A, Walter F, Blitz L, Brinks E, de Blok WJG, Madore B (2010) Extremely Inefficient Star Formation in the Outer Disks of Nearby Galaxies. *AJ*140:1194–1213, DOI 10.1088/0004-6256/140/5/1194, 1007.3498
- Binney J, Tremaine S (1987) *Galactic dynamics*. Princeton, NJ, Princeton University Press
- Binney J, Tremaine S (2008) *Galactic Dynamics: Second Edition*. *Galactic Dynamics: Second Edition*, by James Binney and Scott Tremaine. ISBN 978-0-691-13026-2 (HB). Published by Princeton University Press, Princeton, NJ USA, 2008.
- Bland-Hawthorn J, Vlajić M, Freeman KC, Draine BT (2005) NGC 300: An Extremely Faint, Outer Stellar Disk Observed to 10 Scale Lengths. *ApJ*629:239–249, DOI 10.1086/430512, arXiv:astro-ph/0503488
- Borlaff A, Eliche-Moral MC, Rodríguez-Pérez C, Querejeta M, Tapia T, Pérez-González PG, Zamorano J, Gallego J, Beckman J (2014) Formation of S0 galaxies through mergers. Antitruncated stellar discs resulting from major mergers. *A&A*570:A103, DOI 10.1051/0004-6361/201424299, 1407.5097
- Bournaud F, Elmegreen BG, Elmegreen DM (2007) Rapid Formation of Exponential Disks and Bulges at High Redshift from the Dynamical Evolution of Clump-Cluster and Chain Galaxies. *ApJ*670:237–248, DOI 10.1086/522077, 0708.0306
- Bovy J, Rix HW, Schlafly EF, Nidever DL, Holtzman JA, Shetrone M, Beers TC (2016) The Stellar Population Structure of the Galactic Disk. *ApJ*823:30, DOI 10.3847/0004-637X/823/1/30, 1509.05796
- Braun R, Thilker DA (2004) The WSRT wide-field H I survey. II. Local Group features. *A&A*417:421–435, DOI 10.1051/0004-6361:20034423, astro-ph/0312323
- Brunetti M, Chiappini C, Pfenniger D (2011) Stellar diffusion in barred spiral galaxies. *A&A*534:A75, DOI 10.1051/0004-6361/201117566, 1108.5631
- Byrd G, Rautiainen P, Salo H, Buta R, Crocher DA (1994) Pattern speed domains in ringed disk galaxies from observational and simulational databases. *AJ*108:476–490, DOI 10.1086/117085
- Byun YI (1998) Surface photometry of edge-on galaxies: IC 5249 and ESO 404-G18. *Chinese Journal of Physics* 36:677–692
- Chiappini C, Matteucci F, Gratton R (1997) The Chemical Evolution of the Galaxy: The Two-Infall Model. *ApJ*477:765–780, astro-ph/9609199
- Christlein D, Zaritsky D (2008) The Kinematic Properties of the Extended Disks of Spiral Galaxies: A Sample of Edge-on Galaxies. *ApJ*680:1053-1071, DOI 10.1086/587468, 0803.2225

- Christlein D, Zaritsky D, Bland-Hawthorn J (2010) A spectroscopic study of the H $\alpha$  surface brightness profiles in the outer discs of galaxies. *MNRAS*405:2549–2560, DOI 10.1111/j.1365-2966.2010.16631.x, 1003.4872
- Clarke AJ, Debattista VP, Roškar R, Quinn T (2017) The origin of type I profiles in cluster lenticulars: an interplay between ram pressure stripping and tidally induced spiral migration. *MNRAS*465:L79–L83, DOI 10.1093/mnras/slw214, 1610.04030
- Comerón S, Elmegreen BG, Salo H, Laurikainen E, Athanassoula E, Bosma A, Knapen JH, Gadotti DA, Sheth K, Hinz JL, Regan MW, Gil de Paz A, Muñoz-Mateos JC, Menéndez-Delmestre K, Seibert M, Kim T, Mizusawa T, Laine J, Ho LC, Holwerda B (2012) Breaks in Thin and Thick Disks of Edge-on Galaxies Imaged in the Spitzer Survey Stellar Structure in Galaxies (S<sup>4</sup>G). *ApJ*759:98, DOI 10.1088/0004-637X/759/2/98, 1209.1513
- Daniel KJ, Wyse RFG (2015) Constraints on radial migration in spiral galaxies - I. Analytic criterion for capture at corotation. *MNRAS*447:3576–3592, DOI 10.1093/mnras/stu2683, 1412.6110
- Davidge TJ, Puzia TH (2011) The Stellar Archeology of the M33 Disk: Recent Star-forming History and Constraints on the Timing of an Interaction with M31. *ApJ*738:144, DOI 10.1088/0004-637X/738/2/144, 1107.0077
- de Grijs R, Kregel M, Wesson KH (2001) Radially truncated galactic discs. *MNRAS*324:1074–1086, DOI 10.1046/j.1365-8711.2001.04380.x, astro-ph/0002523
- de Jong RS (1996) Near-infrared and optical broadband surface photometry of 86 face-on disk dominated galaxies. IV. Using color profiles to study stellar and dust content of galaxies. *A&A*313:377–395, astro-ph/9604010
- de Jong RS, Seth AC, Radburn-Smith DJ, Bell EF, Brown TM, Bullock JS, Courteau S, Dalcanton JJ, Ferguson HC, Goudfrooij P, Holfeltz S, Holwerda BW, Purcell C, Sick J, Zucker DB (2007) Stellar Populations across the NGC 4244 Truncated Galactic Disk. *ApJ*667:L49–L52, DOI 10.1086/522035, 0708.0826
- Debattista VP, Mayer L, Carollo CM, Moore B, Wadsley J, Quinn T (2006) The Secular Evolution of Disk Structural Parameters. *ApJ*645:209–227, DOI 10.1086/504147, astro-ph/0509310
- Eliche-Moral MC, Borlaff A, Beckman JE, Gutiérrez L (2015) Photometric scaling relations of anti-truncated stellar discs in S0-Scd galaxies. *A&A*580:A33, DOI 10.1051/0004-6361/201424692, 1505.04797
- Elmegreen BG, Hunter DA (2006) Radial Profiles of Star Formation in the Far Outer Regions of Galaxy Disks. *ApJ*636:712–720, DOI 10.1086/498082, astro-ph/0509190
- Erwin P, Beckman JE, Pohlen M (2005) Antitruncation of Disks in Early-Type Barred Galaxies. *ApJ*626:L81–L84, DOI 10.1086/431739, arXiv:astro-ph/0505216
- Erwin P, Pohlen M, Beckman JE (2008) The Outer Disks of Early-Type Galaxies. I. Surface-Brightness Profiles of Barred Galaxies. *AJ*135:20–54, DOI 10.1088/0004-6256/135/1/20, 0709.3505

- Erwin P, Gutiérrez L, Beckman JE (2012) A Strong Dichotomy in S0 Disk Profiles between the Virgo Cluster and the Field. *ApJ*744:L11, DOI 10.1088/2041-8205/744/1/L11, 1111.5027
- Fall SM, Efstathiou G (1980) Formation and rotation of disc galaxies with haloes. *MNRAS*193:189–206, DOI 10.1093/mnras/193.2.189
- Ferguson A, Irwin M, Chapman S, Ibata R, Lewis G, Tanvir N (2007) Resolving the Stellar Outskirts of M31 and M33. *Astrophysics and Space Science Proceedings* 3:239, DOI 10.1007/978-1-4020-5573-7-39, astro-ph/0601121
- Ferguson AMN, Wyse RFG, Gallagher JS, Hunter DA (1998) Discovery of Recent Star Formation in the Extreme Outer Regions of Disk Galaxies. *ApJ*506:L19–L22, DOI 10.1086/311626, astro-ph/9808151
- Foyle K, Courteau S, Thacker RJ (2008) An N-body/SPH study of isolated galaxy mass density profiles. *MNRAS*386:1821–1844, DOI 10.1111/j.1365-2966.2008.13201.x, 0803.2716
- Freeman KC (1970) On the Disks of Spiral and so Galaxies. *ApJ*160:811–+
- Gil de Paz A, Madore BF, Boissier S, Swaters R, Popescu CC, Tuffs RJ, Sheth K, Kennicutt RC Jr, Bianchi L, Thilker D, Martin DC (2005) Discovery of an Extended Ultraviolet Disk in the Nearby Galaxy NGC 4625. *ApJ*627:L29–L32, DOI 10.1086/432054, arXiv:astro-ph/0506357
- Gogarten SM, Dalcanton JJ, Williams BF, Roškar R, Holtzman J, Seth AC, Dolphin A, Weisz D, Cole A, Debattista VP, Gilbert KM, Olsen K, Skillman E, de Jong RS, Karachentsev ID, Quinn TR (2010) The Advanced Camera for Surveys Nearby Galaxy Survey Treasury. V. Radial Star Formation History of NGC 300. *ApJ*712:858–874, DOI 10.1088/0004-637X/712/2/858, 1002.1743
- Grand RJJ, Kawata D, Cropper M (2012) The dynamics of stars around spiral arms. *MNRAS*421:1529–1538, DOI 10.1111/j.1365-2966.2012.20411.x, 1112.0019
- Guo Q, White S, Boylan-Kolchin M, De Lucia G, Kauffmann G, Lemson G, Li C, Springel V, Weinmann S (2011) From dwarf spheroidals to cD galaxies: simulating the galaxy population in a  $\Lambda$ CDM cosmology. *MNRAS*413:101–131, DOI 10.1111/j.1365-2966.2010.18114.x, 1006.0106
- Gutiérrez L, Erwin P, Aladro R, Beckman JE (2011) The Outer Disks of Early-type Galaxies. II. Surface-brightness Profiles of Unbarred Galaxies and Trends with Hubble Type. *AJ*142:145, DOI 10.1088/0004-6256/142/5/145, 1108.3662
- Halle A, Di Matteo P, Haywood M, Combes F (2015) Quantifying stellar radial migration in an N-body simulation: blurring, churning, and the outer regions of galaxy discs. *A&A*578:A58, DOI 10.1051/0004-6361/201525612, 1501.00664
- Hayden MR, Bovy J, Holtzman JA, Nidever DL, Bird JC, Weinberg DH, Andrews BH, Allende Prieto C, Anders F, Beers TC, Bizyaev D, Chiappini C, Cunha K, Frinchaboy P, García-Herrández DA, García Pérez AE, Girardi L, Harding P, Hearty FR, Johnson JA, Majewski SR, Mészáros S, Minchev I, O’Connell R, Pan K, Robin AC, Schiavon RP, Schneider DP, Schultheis M, Shetrone M, Skrutskie M, Steinmetz M, Smith V, Zamora O, Zasowski G (2015) Chemical Cartography with APOGEE: Metallicity Distribution Functions and the Chemical Structure of

- the Milky Way Disk. *ApJ*808:132, DOI 10.1088/0004-637X/808/2/132, 1503.02110
- Haywood M, Di Matteo P, Lehnert MD, Katz D, Gómez A (2013) The age structure of stellar populations in the solar vicinity. Clues of a two-phase formation history of the Milky Way disk. *A&A*560:A109, DOI 10.1051/0004-6361/201321397, 1305.4663
- Herpich J, Stinson GS, Dutton AA, Rix HW, Martig M, Roškar R, Macciò AV, Quinn TR, Wadsley J (2015a) How to bend galaxy disc profiles: the role of halo spin. *MNRAS*448:L99–L103, DOI 10.1093/mnras/rlv006, 1501.01960
- Herpich J, Stinson GS, Rix HW, Martig M, Dutton AA (2015b) How to bend galaxy disc profiles II: stars surfing the bar in anti-truncated discs. *ArXiv e-prints* 1511.04442
- Kazantzidis S, Magorrian J, Moore B (2004) Generating Equilibrium Dark Matter Halos: Inadequacies of the Local Maxwellian Approximation. *ApJ*601:37–46, DOI 10.1086/380192
- Kazantzidis S, Zentner AR, Kravtsov AV, Bullock JS, Debattista VP (2009) Cold Dark Matter Substructure and Galactic Disks. II. Dynamical Effects of Hierarchical Satellite Accretion. *ApJ*700:1896–1920, DOI 10.1088/0004-637X/700/2/1896, 0902.1983
- Kennicutt RC Jr (1989) The star formation law in galactic disks. *ApJ*344:685–703, DOI 10.1086/167834
- Kregel M, van der Kruit PC, de Grijs R (2002) Flattening and truncation of stellar discs in edge-on spiral galaxies. *MNRAS*334:646–668, DOI 10.1046/j.1365-8711.2002.05556.x, astro-ph/0204154
- Kudritzki RP, Urbaneja MA, Bresolin F, Przybilla N, Gieren W, Pietrzyński G (2008) Quantitative Spectroscopy of 24 A Supergiants in the Sculptor Galaxy NGC 300: Flux-weighted Gravity-Luminosity Relationship, Metallicity, and Metallicity Gradient. *ApJ*681:269–289, DOI 10.1086/588647, 0803.3654
- Kuijken K, Dubinski J (1995) Nearly Self-Consistent Disc / Bulge / Halo Models for Galaxies. *MNRAS*277:1341–+
- Laine J, Laurikainen E, Salo H, Comerón S, Buta RJ, Zaritsky D, Athanassoula E, Bosma A, Muñoz-Mateos JC, Gadotti DA, Hinz JL, Erroz-Ferrer S, Gil de Paz A, Kim T, Menéndez-Delmestre K, Mizusawa T, Regan MW, Seibert M, Sheth K (2014) Morphology and environment of galaxies with disc breaks in the S<sup>4</sup>G and NIRS0S. *MNRAS*441:1992–2012, DOI 10.1093/mnras/stu628, 1404.0559
- Larson RB (1976) Models for the formation of disc galaxies. *MNRAS*176:31–52, DOI 10.1093/mnras/176.1.31
- Laurikainen E, Salo H (2001) BVRI imaging of M51-type interacting galaxy pairs - III. Analysis of the photometric parameters. *MNRAS*324:685–698, DOI 10.1046/j.1365-8711.2001.04347.x
- Lemonias JJ, Schiminovich D, Thilker D, Wyder TK, Martin DC, Seibert M, Treyer MA, Bianchi L, Heckman TM, Madore BF, Rich RM (2011) The Space Density of Extended Ultraviolet (XUV) Disks in the Local Universe and Implications for Gas Accretion onto Galaxies. *ApJ*733:74, DOI 10.1088/0004-637X/733/2/74, 1104.4501

- Loebman SR, Debattista VP, Nidever DL, Hayden MR, Holtzman JA, Clarke AJ, Roškar R, Valluri M (2016) Imprints of Radial Migration on the Milky Way's Metallicity Distribution Functions. *ApJ*818:L6, DOI 10.3847/2041-8205/818/1/L6, 1511.06369
- Lynden-Bell D, Kalnajs AJ (1972) On the generating mechanism of spiral structure. *MNRAS*157:1, DOI 10.1093/mnras/157.1.1
- MacArthur LA, Courteau S, Bell E, Holtzman JA (2004) Structure of Disk-dominated Galaxies. II. Color Gradients and Stellar Population Models. *ApJS*152:175–199, DOI 10.1086/383525, astro-ph/0401437
- Maltby DT, Gray ME, Aragón-Salamanca A, Wolf C, Bell EF, Jogee S, Häußler B, Barazza FD, Böhm A, Jahnke K (2012a) The environmental dependence of the structure of outer galactic discs in STAGES spiral galaxies. *MNRAS*419:669–686, DOI 10.1111/j.1365-2966.2011.19727.x, 1108.6206
- Maltby DT, Hoyos C, Gray ME, Aragón-Salamanca A, Wolf C (2012b) Antitruncated stellar light profiles in the outer regions of STAGES spiral galaxies: bulge or disc related? *MNRAS*420:2475–2479, DOI 10.1111/j.1365-2966.2011.20211.x, 1111.3801
- Martin CL, Kennicutt RC Jr (2001) Star Formation Thresholds in Galactic Disks. *ApJ*555:301–321, DOI 10.1086/321452, astro-ph/0103181
- Martín-Navarro I, Bakos J, Trujillo I, Knapen JH, Athanassoula E, Bosma A, Comerón S, Elmegreen BG, Erroz-Ferrer S, Gadotti DA, Gil de Paz A, Hinz JL, Ho LC, Holwerda BW, Kim T, Laine J, Laurikainen E, Menéndez-Delmestre K, Mizusawa T, Muñoz-Mateos JC, Regan MW, Salo H, Seibert M, Sheth K (2012) A unified picture of breaks and truncations in spiral galaxies from SDSS and S<sup>4</sup>G imaging. *MNRAS*427:1102–1134, DOI 10.1111/j.1365-2966.2012.21929.x, 1208.2893
- Martín-Navarro I, Trujillo I, Knapen JH, Bakos J, Fliri J (2014) Stellar haloes outshine disc truncations in low-inclined spirals. *MNRAS*441:2809–2814, DOI 10.1093/mnras/stu767, 1401.3749
- Matteucci F, Franco P (1989) Galactic chemical evolution - Abundance gradients of individual elements. *MNRAS*239:885–904
- Minchev I, Famaey B (2010) A New Mechanism for Radial Migration in Galactic Disks: Spiral-Bar Resonance Overlap. *ApJ*722:112–121, DOI 10.1088/0004-637X/722/1/112, 0911.1794
- Minchev I, Famaey B, Combes F, Di Matteo P, Mouhcine M, Wozniak H (2011) Radial migration in galactic disks caused by resonance overlap of multiple patterns: Self-consistent simulations. *A&A*527:A147, DOI 10.1051/0004-6361/201015139, 1006.0484
- Minchev I, Famaey B, Quillen AC, Di Matteo P, Combes F, Vlajić M, Erwin P, Bland-Hawthorn J (2012) Evolution of galactic discs: multiple patterns, radial migration, and disc outskirts. *A&A*548:A126, DOI 10.1051/0004-6361/201219198, 1203.2621
- Mo HJ, Mao S, White SDM (1998) The formation of galactic discs. *MNRAS*295:319–336, DOI 10.1046/j.1365-8711.1998.01227.x, astro-ph/9707093

- Muñoz-Mateos JC, Gil de Paz A, Boissier S, Zamorano J, Jarrett T, Gallego J, Madore BF (2007) Specific Star Formation Rate Profiles in Nearby Spiral Galaxies: Quantifying the Inside-Out Formation of Disks. *ApJ*658:1006–1026, DOI 10.1086/511812, [arXiv:astro-ph/0612017](https://arxiv.org/abs/astro-ph/0612017)
- Muñoz-Mateos JC, Sheth K, Gil de Paz A, Meidt S, Athanassoula E, Bosma A, Comerón S, Elmegreen DM, Elmegreen BG, Erroz-Ferrer S, Gadotti DA, Hinz JL, Ho LC, Holwerda B, Jarrett TH, Kim T, Knapen JH, Laine J, Laurikainen E, Madore BF, Menendez-Delmestre K, Mizusawa T, Regan M, Salo H, Schinnerer E, Seibert M, Skibba R, Zaritsky D (2013) The Impact of Bars on Disk Breaks as Probed by S<sup>4</sup>G Imaging. *ApJ*771:59, DOI 10.1088/0004-637X/771/1/59, 1304.6083
- Naab T, Ostriker JP (2006) A simple model for the evolution of disc galaxies: the Milky Way. *MNRAS*366:899–917, DOI 10.1111/j.1365-2966.2005.09807.x, [astro-ph/0505594](https://arxiv.org/abs/astro-ph/0505594)
- Naeslund M, Joersaeter S (1997) Surface photometry of the edge-on spiral NGC 4565. I. V-band data and the extended optical warp. *A&A*325:915–922
- Peñarrubia J, McConnachie A, Babul A (2006) On the Formation of Extended Galactic Disks by Tidally Disrupted Dwarf Galaxies. *ApJ*650:L33–L36, DOI 10.1086/508656, [astro-ph/0606101](https://arxiv.org/abs/astro-ph/0606101)
- Pérez I (2004) Truncation of stellar disks in galaxies at  $z \sim 1$ . *A&A*427:L17–L20, DOI 10.1051/0004-6361:200400090, [astro-ph/0410250](https://arxiv.org/abs/astro-ph/0410250)
- Pohlen M (2002) The Radial Structure of Galactic Stellar Disks. PhD Thesis, Ruhr-Universität
- Pohlen M, Trujillo I (2006) The structure of galactic disks. Studying late-type spiral galaxies using SDSS. *A&A*454:759–772, DOI 10.1051/0004-6361:20064883, [arXiv:astro-ph/0603682](https://arxiv.org/abs/astro-ph/0603682)
- Pohlen M, Dettmar RJ, Lütticke R (2000) Cut-off radii of galactic disks . A new statistical study on the truncation of galactic disks. *A&A*357:L1–L4, [arXiv:astro-ph/0003384](https://arxiv.org/abs/astro-ph/0003384)
- Pohlen M, Dettmar RJ, Lütticke R, Aronica G (2002) Outer edges of face-on spiral galaxies. Deep optical imaging of NGC 5923, UGC 9837 and NGC 5434. *A&A*392:807–816, DOI 10.1051/0004-6361:20020994
- Pranger F, Trujillo I, Kelvin LS, Cebrián M (2016) The effect of environment on the structure of disk galaxies. *ArXiv e-prints* 1605.08845
- Putman ME, Peek JEG, Muratov A, Gnedin OY, Hsu W, Douglas KA, Heiles C, Stanimirovic S, Korpela EJ, Gibson SJ (2009) The Disruption and Fueling of M33. *ApJ*703:1486–1501, DOI 10.1088/0004-637X/703/2/1486, 0812.3093
- Radburn-Smith DJ, de Jong RS, Seth AC, Bailin J, Bell EF, Brown TM, Bullock JS, Courteau S, Dalcanton JJ, Ferguson HC, Goudfrooij P, Holfeltz S, Holwerda BW, Purcell C, Sick J, Streich D, Vlajic M, Zucker DB (2011) The GHOSTS Survey. I. Hubble Space Telescope Advanced Camera for Surveys Data. *ApJS*195:18, DOI 10.1088/0067-0049/195/2/18
- Radburn-Smith DJ, Roškar R, Debattista VP, Dalcanton JJ, Streich D, de Jong RS, Vlajić M, Holwerda BW, Purcell CW, Dolphin AE, Zucker DB (2012) Outer-disk

- Populations in NGC 7793: Evidence for Stellar Radial Migration. *ApJ*753:138, DOI 10.1088/0004-637X/753/2/138, 1206.1057
- Rautiainen P, Salo H (2000) N-body simulations of resonance rings in galactic disks. *A&A*362:465–586
- Rebassa-Mansergas A, Anguiano B, García-Berro E, Freeman KC, Cojocaru R, Manser CJ, Pala AF, Gänsicke BT, Liu XW (2016) The age-metallicity relation in the solar neighbourhood from a pilot sample of white dwarf-main sequence binaries. *MNRAS*463:1137–1143, DOI 10.1093/mnras/stw2021, 1608.03064
- Roca-Fàbrega S, Valenzuela O, Figueras F, Romero-Gómez M, Velázquez H, Antoja T, Pichardo B (2013) On galaxy spiral arms' nature as revealed by rotation frequencies. *MNRAS*432:2878–2885, DOI 10.1093/mnras/stt643, 1302.6981
- Roediger JC, Courteau S, Sánchez-Blázquez P, McDonald M (2012) Stellar Populations and Radial Migrations in Virgo Disk Galaxies. *ApJ*758:41, DOI 10.1088/0004-637X/758/1/41, 1201.6361
- Roškar R, Debattista VP, Quinn TR, Stinson GS, Wadsley J (2008a) Riding the Spiral Waves: Implications of Stellar Migration for the Properties of Galactic Disks. *ApJ*684:L79–L82, DOI 10.1086/592231, 0808.0206
- Roškar R, Debattista VP, Stinson GS, Quinn TR, Kaufmann T, Wadsley J (2008b) Beyond Inside-Out Growth: Formation and Evolution of Disk Outskirts. *ApJ*675:L65–L68, DOI 10.1086/586734, 0710.5523
- Roškar R, Debattista VP, Brooks AM, Quinn TR, Brook CB, Governato F, Dalcanton JJ, Wadsley J (2010) Misaligned angular momentum in hydrodynamic cosmological simulations: warps, outer discs and thick discs. *MNRAS*408:783–796, DOI 10.1111/j.1365-2966.2010.17178.x, 1006.1659
- Roškar R, Debattista VP, Quinn TR, Wadsley J (2012) Radial migration in disc galaxies - I. Transient spiral structure and dynamics. *MNRAS*426:2089–2106, DOI 10.1111/j.1365-2966.2012.21860.x, 1110.4413
- Ruiz-Lara T, Few CG, Gibson BK, Pérez I, Florido E, Minchev I, Sánchez-Blázquez P (2016a) The imprint of satellite accretion on the chemical and dynamical properties of disc galaxies. *A&A*586:A112, DOI 10.1051/0004-6361/201526470, 1512.00625
- Ruiz-Lara T, Pérez I, Florido E, Sánchez-Blázquez P, Méndez-Abreu J, Lyubenova M, Falcón-Barroso J, Sánchez-Menguiano L, Sánchez SF, Galbany L, García-Benito R, González Delgado RM, Husemann B, Kehrig C, López-Sánchez ÁR, Marino RA, Mast D, Papaderos P, van de Ven G, Walcher CJ, Zibetti S, CALIFA Team (2016b) No direct coupling between bending of galaxy disc stellar age and light profiles. *MNRAS*456:L35–L39, DOI 10.1093/mnras/slv174, 1511.03499
- Sánchez-Blázquez P, Courty S, Gibson BK, Brook CB (2009) The origin of the light distribution in spiral galaxies. *MNRAS*398:591–606, DOI 10.1111/j.1365-2966.2009.15133.x, 0905.4579
- Sánchez-Blázquez P, Rosales-Ortega FF, Méndez-Abreu J, Pérez I, Sánchez SF, Zibetti S, Aguerri JAL, Bland-Hawthorn J, Catalán-Torrecilla C, Cid Fernandes R, de Amorim A, de Lorenzo-Caceres A, Falcón-Barroso J, Galazzi A, García Benito R, Gil de Paz A, González Delgado R, Husemann B, Iglesias-Páramo J, Jung-

- wiert B, Marino RA, Márquez I, Mast D, Mendoza MA, Mollá M, Papaderos P, Ruiz-Lara T, van de Ven G, Walcher CJ, Wisotzki L (2014) Stellar population gradients in galaxy discs from the CALIFA survey. The influence of bars. *A&A*570:A6, DOI 10.1051/0004-6361/201423635, 1407.0002
- Schaye J (2004) Star Formation Thresholds and Galaxy Edges: Why and Where. *ApJ*609:667–682, DOI 10.1086/421232, arXiv:astro-ph/0205125
- Schönrich R, Binney J (2009) Chemical evolution with radial mixing. *MNRAS*396:203–222, DOI 10.1111/j.1365-2966.2009.14750.x, 0809.3006
- Schwarz MP (1981) The response of gas in a galactic disk to bar forcing. *ApJ*247:77–88, DOI 10.1086/159011
- Sellwood JA (2011) The lifetimes of spiral patterns in disc galaxies. *MNRAS*410:1637–1646, DOI 10.1111/j.1365-2966.2010.17545.x, 1008.2737
- Sellwood JA (2014) GALAXY package for N-body simulation. ArXiv e-prints 1406.6606
- Sellwood JA, Binney JJ (2002) Radial mixing in galactic discs. *MNRAS*336:785–796, DOI 10.1046/j.1365-8711.2002.05806.x
- Sellwood JA, Carlberg RG (1984) Spiral instabilities provoked by accretion and star formation. *ApJ*282:61–74, DOI 10.1086/162176
- Sellwood JA, Carlberg RG (2014) Transient Spirals as Superposed Instabilities. *ApJ*785:137, DOI 10.1088/0004-637X/785/2/137, 1403.1135
- Sellwood JA, Debattista VP (2009) Stochasticity in N-body simulations of disc galaxies. *MNRAS*398:1279–1297, DOI 10.1111/j.1365-2966.2009.15219.x, 0903.3554
- Shen J, Sellwood JA (2004) The Destruction of Bars by Central Mass Concentrations. *ApJ*604:614–631
- Solway M, Sellwood JA, Schönrich R (2012) Radial migration in galactic thick discs. *MNRAS*422:1363–1383, DOI 10.1111/j.1365-2966.2012.20712.x, 1202.1418
- Thilker DA, Bianchi L, Boissier S, Gil de Paz A, Madore BF, Martin DC, Meurer GR, Neff SG, Rich RM, Schiminovich D, Seibert M, Wyder TK, Barlow TA, Byun YI, Donas J, Forster K, Friedman PG, Heckman TM, Jelinsky PN, Lee YW, Malina RF, Milliard B, Morrissey P, Siegmund OHW, Small T, Szalay AS, Welsh BY (2005) Recent Star Formation in the Extreme Outer Disk of M83. *ApJ*619:L79–L82, DOI 10.1086/425251, arXiv:astro-ph/0411306
- Trujillo I, Pohlen M (2005) Stellar Disk Truncations at High z: Probing Inside-Out Galaxy Formation. *ApJ*630:L17–L20, DOI 10.1086/491472, astro-ph/0507533
- van der Kruit PC (1979) Optical surface photometry of eight spiral galaxies studied in Westerbork. *A&AS*38:15–38
- van der Kruit PC (1987) The radial distribution of surface brightness in galactic disks. *A&A*173:59–80
- van der Kruit PC (1988) The three-dimensional distribution of light and mass in disks of spiral galaxies. *A&A*192:117–127

- van der Kruit PC (2007) Truncations of stellar disks and warps of HI-layers in edge-on spiral galaxies. *A&A*466:883–893, DOI 10.1051/0004-6361:20066941, arXiv:astro-ph/0702486
- van der Kruit PC, Searle L (1982) Surface photometry of edge-on spiral galaxies. IV - The distribution of light, colour, and mass in the disk and spheroid of NGC 7814. *A&A*110:79–94
- Vera-Ciro C, D’Onghia E (2016) On the Conservation of the Vertical Action in Galactic Disks. *ApJ*824:39, DOI 10.3847/0004-637X/824/1/39
- Vlajić M, Bland-Hawthorn J, Freeman KC (2009) The Abundance Gradient in the Extremely Faint Outer Disk of NGC 300. *ApJ*697:361–372, DOI 10.1088/0004-637X/697/1/361, 0903.1855
- Watkins AE, Mihos JC, Harding P, Feldmeier JJ (2014) Searching for Diffuse Light in the M96 Galaxy Group. *ApJ*791:38, DOI 10.1088/0004-637X/791/1/38, 1406.6982
- Watkins AE, Mihos JC, Harding P (2016) The Red and Featureless Outer Disks of Nearby Spiral Galaxies. *ApJ*826:59, DOI 10.3847/0004-637X/826/1/59, 1605.05183
- Widrow LM, Dubinski J (2005) Equilibrium Disk-Bulge-Halo Models for the Milky Way and Andromeda Galaxies. *ApJ*631:838–855, DOI 10.1086/432710
- Widrow LM, Pym B, Dubinski J (2008) Dynamical Blueprints for Galaxies. *ApJ*679:1239–1259, DOI 10.1086/587636, 0801.3414
- Williams BF, Dalcanton JJ, Dolphin AE, Holtzman J, Sarajedini A (2009) The Detection of Inside-Out Disk Growth in M33. *ApJ*695:L15–L19, DOI 10.1088/0004-637X/695/1/L15, 0902.3460
- Williams BF, Dalcanton JJ, Stilp A, Dolphin A, Skillman ED, Radburn-Smith D (2013) The ACS Nearby Galaxy Survey Treasury. XI. The Remarkably Undisturbed NGC 2403 Disk. *ApJ*765:120, DOI 10.1088/0004-637X/765/2/120, 1301.4521
- Worthey G (1994) Comprehensive stellar population models and the disentanglement of age and metallicity effects. *ApJS*95:107–149, DOI 10.1086/192096
- Yoachim P, Roškar R, Debattista VP (2012) Spatially Resolved Spectroscopic Star Formation Histories of nearby Disks: Hints of Stellar Migration. *ApJ*752:97, DOI 10.1088/0004-637X/752/2/97, 1204.0026
- Younger JD, Cox TJ, Seth AC, Hernquist L (2007) Antitruncated Stellar Disks via Minor Mergers. *ApJ*670:269–278, DOI 10.1086/521976, 0707.4481
- Yu J, Sellwood JA, Pryor C, Chen L, Hou J (2012) A Test for Radial Mixing Using Local Star Samples. *ApJ*754:124, DOI 10.1088/0004-637X/754/2/124, 1205.7001
- Zaritsky D, Christlein D (2007) On the Extended Knotted Disks of Galaxies. *AJ*134:135–141, DOI 10.1086/518238, astro-ph/0703487
- Zheng Z, Thilker DA, Heckman TM, Meurer GR, Burgett WS, Chambers KC, Huber ME, Kaiser N, Magnier EA, Metcalfe N, Price PA, Tonry JL, Wainscoat RJ, Waters C (2015) The Structure and Stellar Content of the Outer Disks of Galaxies: A New View from the Pan-STARRS1 Medium Deep Survey. *ApJ*800:120, DOI 10.1088/0004-637X/800/2/120, 1412.3209